Human Molecular Genetics, 2014, Vol. 23, No. 4 **889–905**
doi:10.1093/hmg/ddt484
Advance Access published on October 1, 2013

WNT/β-catenin signalling is activated in aldosterone-producing adenomas and controls aldosterone production

Annabel Berthon[1,2,3], Coralie Drelon[1,2,3], Bruno Ragazzon[4,5,†], Sheerazed Boulkroun[6,7,†], Frédérique Tissier[4,5,8,9], Laurence Amar[6,7,10], Benoît Samson-Couterie[6,7], Maria-Christina Zennaro[6,7,11], Pierre-François Plouin[6,7,10], Seham Skah[12], Michelina Plateroti[12], Hervé Lefèbvre[13,14], Isabelle Sahut-Barnola[1,2,3], Marie Batisse-Lignier[1,2,3,15], Guillaume Assié[4,5,16], Anne-Marie Lefrançois-Martinez[1,2,3], Jérôme Bertherat[4,5,16], Antoine Martinez[1,2,3] and Pierre Val[1,2,3,*]

[1]Clermont Université, Université Blaise Pascal, GReD, BP 10448, F-63000 Clermont-Ferrand, France, [2]CNRS, UMR 6293, GReD, F-63001 Clermont-Ferrand, France, [3]Inserm, UMR 1103, GReD, F-63001 Clermont-Ferrand, France, [4]Institut Cochin, Université Paris Descartes, CNRS (UMR 8104), Paris, F-75014, [5]Inserm, U1016, Paris, F-75014, [6]Institut National de la Santé et de la recherche médicale, UMRS_970, Paris Cardiovascular Research Center, [7]Université Paris Descartes, Sorbonne Paris Cité, Paris, France, [8]Department of Pathology, Pitie-Salpetriere Hospital, AP-HP, Pierre and Marie Curie University, [9]Department of Pathology, Cochin Hospital, AP-HP, Paris, France, [10]Assistance Publique-Hôpitaux de Paris, Hôpital Européen Georges Pompidou, Unité Hypertension artérielle, Paris, France, [11]Assistance Publique-Hôpitaux de Paris, Hôpital Européen Georges Pompidou, Service de Génétique, Paris, France, [12]CNRS, UMR 5534, F-69622 Villeurbanne, [13]Institut National de la Santé et de la Recherche Médicale Unité 982, and University of Rouen, F-76821 Mont-Saint Aignan, [14]University Hospital of Rouen, F-76031 Rouen, [15]Centre Hospitalier Universitaire, Service d'Endocrinologie, Faculté de Médecine, Clermont-Ferrand, F-63000 and [16]Assistance Publique Hôpitaux de Paris, Hôpital Cochin, Department of Endocrinology, Reference Center for Rare Adrenal Diseases, Paris, F-75014

Received July 26, 2013; Revised September 13, 2013; Accepted September 24, 2013

Primary aldosteronism (PA) is the main cause of secondary hypertension, resulting from adrenal aldosterone-producing adenomas (APA) or bilateral hyperplasia. Here, we show that constitutive activation of WNT/β-catenin signalling is the most frequent molecular alteration found in 70% of APA. We provide evidence that decreased expression of the WNT inhibitor *SFRP2* may be contributing to deregulated WNT signalling and APA development in patients. This is supported by the demonstration that mice with genetic ablation of *Sfrp2* have increased aldosterone production and ectopic differentiation of zona glomerulosa cells. We further show that β-catenin plays an essential role in the control of basal and Angiotensin II-induced aldosterone secretion, by activating *AT1R*, *CYP21* and *CYP11B2* transcription. This relies on both LEF/TCF-dependent activation of *AT1R* and *CYP21* regulatory regions and indirect activation of *CYP21* and *CYP11B2* promoters, through increased expression of the nuclear receptors NURR1 and NUR77. Altogether, these data show that aberrant WNT/β-catenin activation is associated with APA development and suggest that WNT pathway may be a good therapeutic target in PA.

INTRODUCTION

Adrenal autonomous secretion of aldosterone also called primary aldosteronism (PA) is the main cause of secondary hypertension with a prevalence of 6–13% of hypertensive patients (1,2). In 95% of the cases, this pathology is caused by adrenal aldosterone-producing adenomas (APA) or bilateral hyperplasia (3). Clinical management of PA essentially relies

*To whom correspondence should be addressed at: Pierre VAL, CNRS UMR 6293 GReD, 24 avenue des Landais, 63171 Aubiere Cedex, France. Tel: + 33 473407412; Fax: +33 473407042; Email: pierre.val@univ-bpclermont.fr
†The authors wish it to be known that, in their opinion, the third and fourth authors should be regarded as joint third authors.

on surgical resection and/or treatment with mineralocorticoids antagonists to minimize hypertension (4,5). However, complete normalization of blood pressure is rarely achieved and mineralocorticoids antagonists are associated with adverse endocrine side effects (6). Although new promising treatments such as aldosterone synthase inhibitors are emerging (7,8), identification of the molecular aetiology of PA is essential to allow the development of more specific and more efficient drugs. Multiple molecular alterations such as down-regulation of TASK channels (9,10) or circadian clock deregulation (11) have been proposed to play a role in the establishment of PA but their clinical relevance is still unclear. Recent data suggest that the development of a subset of APA is associated with mutations in the *KCNJ5* gene, which cause dysfunction of the Kir3.4 potassium channel, or mutations in the genes encoding the ATPases ATP1A1 and ATP2B3 (12–16). In both cases, these alterations result in inappropriate membrane depolarization, which increases steroidogenic capacities of adrenocortical cells. Even though *KCNJ5* and ATPases mutations account for ∼40–45% of patients with sporadic PA, the molecular mechanisms underlying the majority of APA still remain elusive (13,15,16,17,18).

We have recently shown that transgenic mice with specific constitutive activation of β-catenin in the adrenal cortex presented with increased aldosterone production (19). Here, we have investigated the hypothesis that aberrant WNT pathway activation may play a role in the development of APA in patients.

RESULTS

WNT/β-catenin pathway is constitutively activated in APA

To evaluate the potential role of WNT pathway in the development of APA, we analysed the status of WNT/β-catenin pathway activation in tissue samples from 47 patients diagnosed with PA caused by adrenal APA. Patients' clinical and biological characteristics are described in Supplementary Material, Table S1A. Immunohistochemistry for β-catenin showed cytoplasmic (Fig. 1Ac and d) and/or nuclear (Fig. 1Ae and f) accumulation of β-catenin in 33/47 APA (Supplementary Material, Table S1B). This suggested that WNT/β-catenin signalling was activated in 70% of APA in our series (Fig. 1A and Supplementary Material, Table S1B). To confirm these observations, WNT/β-catenin pathway target genes expression was analysed by reverse-transcription quantitative polymerase chain reaction (RTqPCR) in 35 out of the 47 APA that were analysed by immunohistochemistry (Supplementary Material, Table S1B). In these experiments, APA were compared with 7 normal adrenals (NA) and 17 non-aldosterone-producing adenomas (NAPA) that were selected on the basis of cortisol or androgen secretion and absence of histological signs of β-catenin activation. These experiments demonstrated a significant overexpression of *AXIN2* (Fig. 1B) and *LEF1* (Fig. 1C) in APA compared with both NA and NAPA. We then analysed expression of *CYP11B2* (Fig. 1D) and performed correlation analyses with *AXIN2* and *LEF1* expression levels. These experiments showed a strong association between *AXIN2* (Fig. 1E), *LEF1* (Fig. 1F) and *CYP11B2* expression levels. To further strengthen our hypothesis of an association between WNT activation and CYP11B2 overexpression, we analysed expression of *CYP11B2* (by *in situ* hybridization) and β-catenin (by immunohistochemistry) on consecutive sections of APA. These data showed that cells within the adenoma displayed both high levels of *CYP11B2* expression (Fig. 1Gb and c) and nuclear β-catenin staining (Fig. 1Gd and e). We therefore concluded that canonical WNT/β-catenin signalling was activated in a majority of APA and that this activation was correlated with increased CYP11B2 expression.

WNT/β-catenin pathway activation in APA is associated with down-regulation of *SFRP2*

WNT/β-catenin pathway activation in adrenal tumours has mostly been attributed to activating mutations in the *CTNNB1* gene (20). However, there were no such mutations in our series of 26 β-catenin-positive APA for which genomic DNA was available (Supplementary Material, Table S1B). This result was in agreement with a recent report showing no activating *CTNNB1* mutations in 41 APA (21). We then evaluated the possibility of an association between WNT pathway activation and *KCNJ5* mutations. Out of the 19 β-catenin-positive tumours that were available for sequencing, 9 were mutant for *KCNJ5* (47%). However, 6/9 (67%) of the β-catenin-negative tumours were also mutant for *KCNJ5* (Supplementary Material, Table S1B). This suggested that there was no association between *KCNJ5* mutations and canonical WNT/β-catenin pathway activation in APA. In an attempt to identify WNT regulators that may be relevant to APA development, we compared expression levels of known WNT regulators (based on a compilation of data available from the Wnt Homepage and PubMed browsing) in six APA and four NA by retrospective analysis of cDNA microarray data ((22), Supplementary Material, Fig. S1). This analysis confirmed significant up-regulation of *AXIN2* and *LEF1* expression in APA, but surprisingly failed to identify up-regulation of positive regulators of WNT pathway activity, with the exception of Lrp6 WNT coreceptor (Supplementary Material, Fig. S1). However, this approach showed significant down-regulation of *SFRP1*, *2* and *4*, three members of the SFRP (secreted frizzled related protein) family of WNT signalling inhibitors, in APA. These factors have the ability to bind and titrate WNT ligands and their down-regulation has been shown to stimulate WNT pathway activation in tumours (23). To further confirm our transcriptome data, we analysed expression of *SFRP1*, *SFRP2* and *SFRP4* by RTqPCR in our series of 35 APA in comparison with NAPA and NA. We reasoned that factors relevant to WNT pathway activation and aldosterone production should be deregulated in APA in comparison with both NA and NAPA. In these experiments, *SFRP1* was down-regulated in APA and NAPA compared with NA (Fig. 2A). However, there was no significant difference in *SFRP1* expression in APA compared with NAPA, suggesting that it was not involved in the establishment of the aldosterone-producing phenotype. In contrast with the microarray data, RTqPCR analyses of our larger series did not show down-regulation of *SFRP4* in APA compared with NA and even showed up-regulation in comparison with NAPA (Fig. 2B). Interestingly, *SFRP2* expression was significantly downregulated in APA compared with both NA and NAPA (Fig. 2C). This suggested that it could be involved in the establishment of deregulated WNT signalling and subsequent aldosteronism in APA patients. Consistent with this idea, *SFRP2*

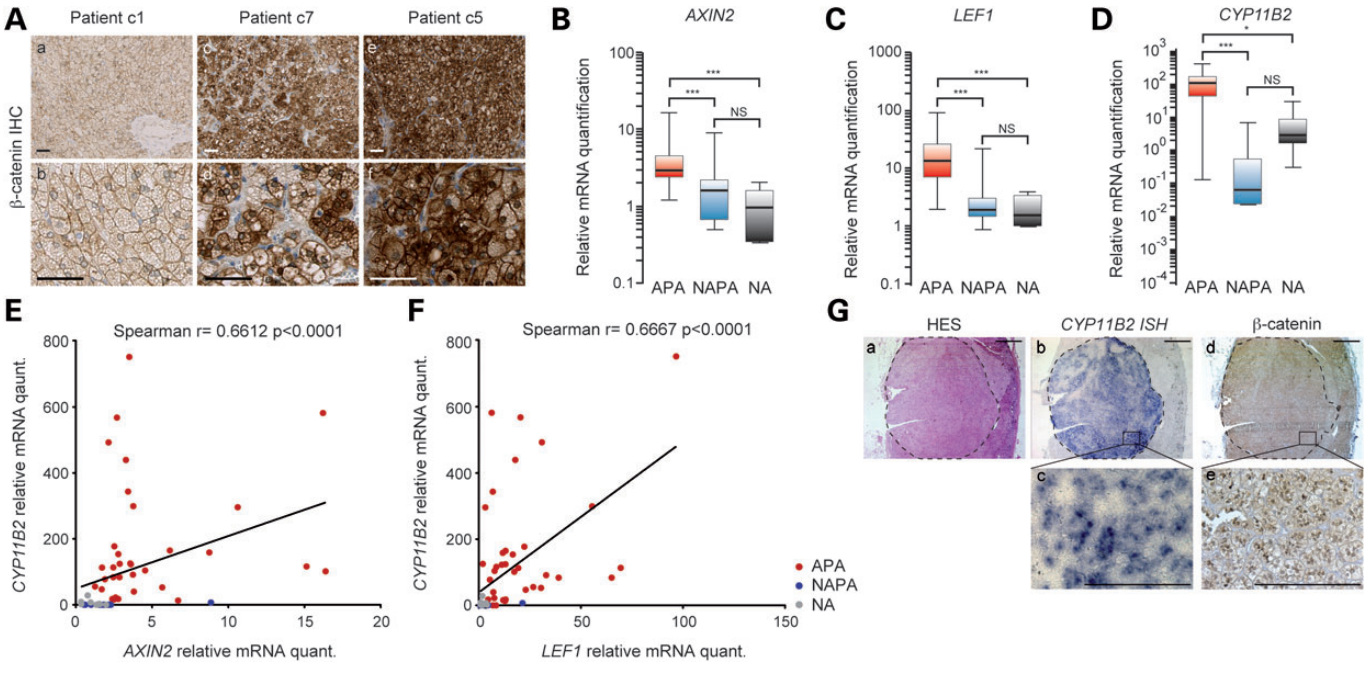

Figure 1. WNT/β-catenin pathway is activated in Conn's syndrome patients. (**A**) Nucleo-cytoplasmic accumulation of β-catenin in APA. Immunohistochemistry shows cytoplasmic (e.g. patient #c7) or nucleocytoplasmic (e.g. patient #c5) accumulation of β-catenin in 33 out of 47 APA and wild-type membrane-associated staining in 14 out of 47 APA (e.g. patient #c1). Scale bar is 200 μm. (**B** and **C**) Two β-catenin target genes, *AXIN2* and *LEF1* are up-regulated in APA. *AXIN2* and *LEF1* expression levels were analysed by RTqPCR on mRNAs from 35 APA, 17 NAPA and 7 NA. (**D**) *CYP11B2* is up-regulated in aldosterone-producing tumours. Aldosterone synthase *CYP11B2* expression was analysed by RTqPCR on mRNAs from APA, NAPA and NA. (**E** and **F**) *AXIN2* and *LEF1* expression levels are correlated with *CYP11B2* expression. RTqPCR data were used to correlate WNT pathway activation (*AXIN2* and *LEF1*) with *CYP11B2* expression in a Spearman correlation analysis. (**G**) CYP11B2 and nuclear β-catenin are expressed in similar areas of APA. *CYP11B2* (*in situ* hybridization, b and c) and β-catenin (immunohistochemistry, d and e) were detected in consecutive sections fromAPA. Haematoxylin-eosin-safran (HES) staining shows the structure of the adenoma within the adrenal cortex (a), delimited by a dashed line. Scale bar is 200 μm in a, b and d and 50 μm in c and e. Statistical analyses in (B)–(D) were performed by non-parametric ANOVA (Kruskal–Wallis) followed by Dunn's *post hoc* test. $^{*}P < 0.05$; $^{**}P < 0.005$; $^{***}P < 0.0005$.

expression was inversely correlated with both *AXIN2* (Supplementary Material, Fig. S2A) and *CYP11B2* expression (Fig. 2D).

Sfrp2 knockout mice have increased Wnt signalling and aldosterone production

To further explore a link between *SFRP2* down-regulation and APA development, we analysed plasma aldosterone concentrations in *Sfrp2* knockout mice. These mice are characterized by brachy-syndactyly, but their adrenal function was never investigated (24). Individual increases in plasma aldosterone were observed as early as 7 months in homozygous mutant females; however, significant overall increases were only observed in 12- to −13-month-old mutants compared with wild-type littermates (Fig. 2E). These were independent of renin, which was not significantly elevated in *Sfrp2* knockout mice (3.77 ± 2.88 mUI/l) compared to wild-type mice (2.38 ± 1.29 mUI/l). The hormonal phenotype was specific of aldosterone, as corticosterone levels were not significantly altered by *Sfrp2* knockout (Supplementary Material, Fig. S2B). Consistent with a role of Sfrp2 in restraining Wnt signalling in the adrenal, mRNA accumulation of *Axin2* (Fig. 2F) and *Lef1* (Fig. 2G) was increased in *Sfrp2*$^{-/-}$ adrenals. Interestingly, plasma aldosterone concentration was significantly correlated with *Axin2* mRNA accumulation (Spearman $r = 0.4834$, $P = 0.0167$). We further confirmed these observations by immunohistochemical analysis of Dab2 (a molecular marker of zona-glomerulosa differentiation (25)), β-catenin and Cyp11b2 expression. Consistent with the endocrine and molecular phenotypes, immunohistological analysis of *Sfrp2* knockout adrenals showed ectopic Dab2 (Fig. 2Hb versus a) and β-catenin-positive cells (Fig. 2He versus d) within the adrenal cortex and central adrenal region. These ectopic cells were also positive for Cyp11b2 (Fig. 2Hh versus g; Supplementary Material, Fig. S2C), which was reminiscent of the phenotype of ΔCat mice with adrenal-specific constitutive β-catenin activation (Fig. 2Hc, f and i (19)). This showed that *Sfrp2* knockout was sufficient to increase adrenal WNT signalling and aldosterone secretion. We thus concluded that down-regulation of *SFRP2* expression was one of the possible causes for deregulation of WNT signalling and development of APA in patients.

β-Catenin controls aldosterone production at multiple levels

In order to understand the role of β-catenin in aldosterone production, we used the human adrenocortical cell line H295R that has the ability to produce aldosterone in response to its natural secretagogue, Angiotensin II. However, it spontaneously expresses a constitutive active mutant form of β-catenin (S45A mutation) (26). We therefore decided to down-regulate β-catenin activity and to assess basal and Angiotensin II-induced aldosterone production. Transfection of H295R cells with small interfering RNAs to β-catenin induced a mean 60% decrease in β-catenin expression compared with unrelated GFP siRNA (Supplementary Material,

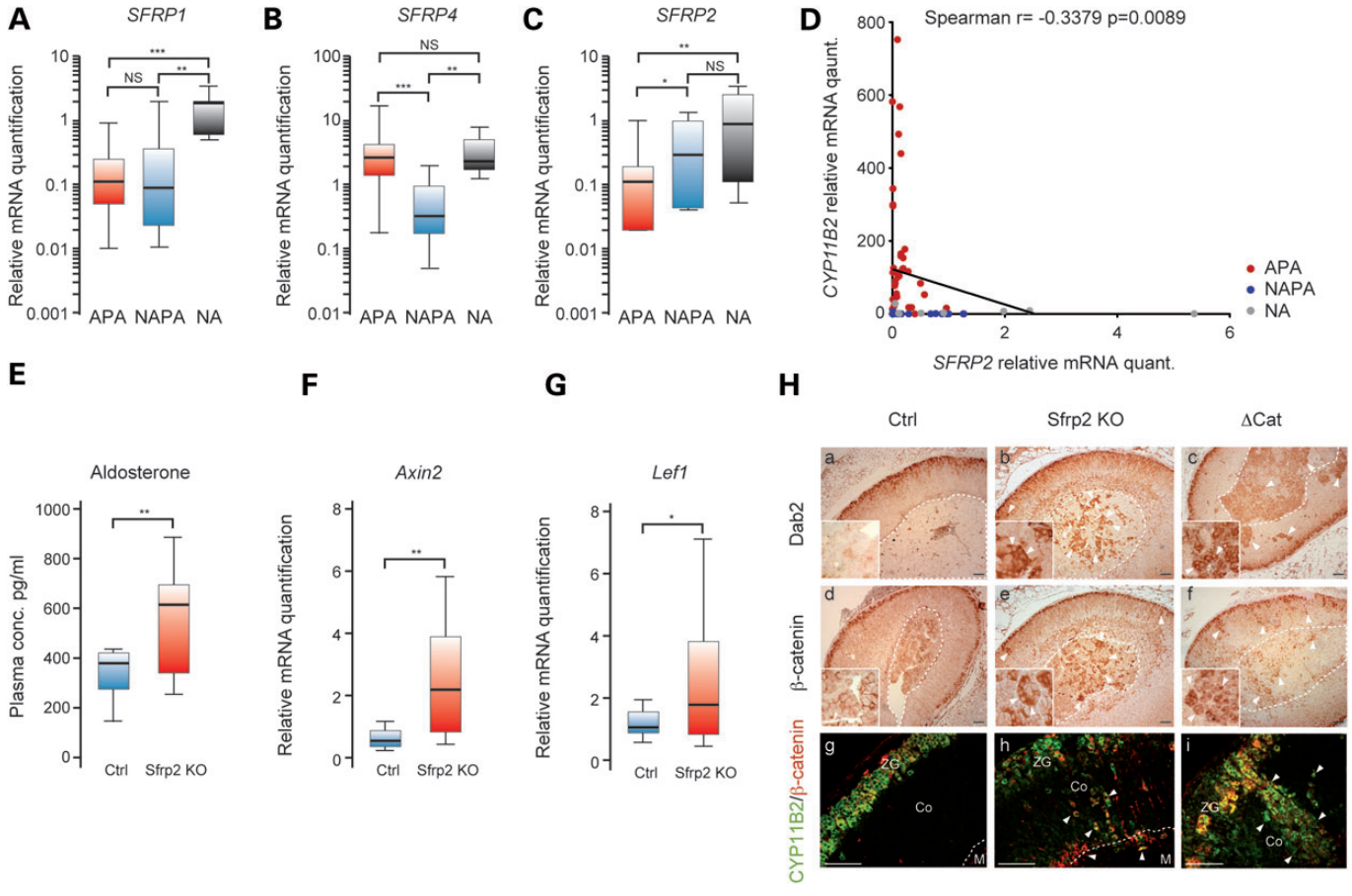

Figure 2. Down-regulation of *SFRP2* expression is associated with WNT pathway activation and aldosteronism. (**A**–**C**) *SFRP2* is down-regulated in APA. The expression of three members of the secreted frizzled related protein (SFRP), *SFRP1*, *SFRP2*, *SFRP4* was analysed by RTqPCR on mRNAs from 35 APA, 17 NAPA and 7 NA. (**D**) SFRP2 and CYP11B2 expression levels are inversely correlated. RTqPCR data were used to correlate *SFRP2* with *CYP11B2* expression in a Spearman correlation analysis. (**E**) *Sfrp2* knockout is associated with increased aldosterone production. Plasma aldosterone concentrations were measured in female control (Ctrl, $Sfrp2^{+/+}$ and $Sfrp2^{+/-}$) and female homozygous *Sfrp2* knockout mice (Sfrp2 KO, $Sfrp2^{-/-}$) at 13 months. Boxplots represent the quantification of aldosterone production in 11 female control and 13 littermate female knockout mice. (**F** and **G**) Wnt signalling is increased in the adrenals of *Sfrp2* knockout mice. *Axin2* (F) and *Lef1* (G) expression levels were analysed by RTqPCR on mRNAs from control and homozygous *Sfrp2* knockout mice. Boxplots represent the relative quantification of gene expression in 11 female control and 13 female knockout mice. (**H**) Genetic ablation of *Sfrp2* results in aberrant activation of β-catenin and ectopic differentiation of zona-glomerulosa cells. Expression of Dab2 (a–c) β-catenin (d–f) and co-expression of β-catenin (red) and Cyp11b2 (green, g–i) was analysed by immunohistochemistry in wild-type ($Sfrp2^{+/+}$), Sfrp2 knockout ($Sfrp2^{-/-}$) and ΔCat mice (19). Insets were taken from the central adrenal regions, highlighted by dashed white lines. White arrowheads show ectopic Cyp11b2, Dab2 and β-catenin-positive cells. Dashed lines show the boundaries between cortex and medulla. ZG, zona glomerulosa; Co, cortex; M, medulla. Scale bar is 80 μm. Statistical analyses in (A)–(C) were performed by non-parametric ANOVA (Kruskal–Wallis) followed by Dunn's *post hoc* test. Statistical analyses in (E)–(G) were performed by Welch's *t*-test, to account for different variances between groups. Similar results were obtained by Mann–Whitney analyses $^{*}P < 0.05$; $^{**}P < 0.005$; $^{***}P < 0.0005$; NS, not significant.

Fig. S3A and B). As expected, this resulted in a significant down-regulation of *AXIN2* (Supplementary Material, Fig. S3C) and *LEF1* (Supplementary Material, Fig. S3D) target gene expression. Interestingly, down-regulation of β-catenin also resulted in a marked decrease in basal aldosterone output and completely abrogated response to Angiotensin II (Fig. 3A). In order to confirm these observations, we treated H295R cells with PKF115-584, a previously published inhibitor of β-catenin transcriptional activity (27). As expected, treatment with PKF115-584 induced a dose-dependent decrease in the expression of *AXIN2* (Supplementary Material, Fig. S3E) and *LEF1* (Supplementary Material, Fig. S3F). Consistent with our siRNA data, this treatment also induced a dose-dependent decrease in basal aldosterone production and markedly reduced Angiotensin II responsiveness at the highest dose (Fig. 3B). We thus concluded that β-catenin was required for basal aldosterone production and that it was essential to mediate Angiotensin II response in H295R cells. To identify relevant β-catenin target genes involved in the control of aldosterone production, we analysed expression of all the genes coding proteins involved in aldosterone synthesis and of the Angiotensin II Type I receptor *AT1R*, by RTqPCR (Fig. 3C). Treatment with β-catenin siRNAs resulted in a decrease in Angiotensin II-induced mRNA accumulation of *CYP11B2* (Fig. 3D) and *CYP21* (Fig. 3E) and inhibition of basal expression of *AT1R* (Fig. 3F). Similar results were obtained in cells treated with PKF115-584 (Fig. 3G–I). In contrast, β-catenin siRNAs had no significant effect on the expression of *StAR*, *CYP11A1*, *HSD3B2* and *CYP11B1* (Supplementary Material, Fig. S3G–J).

To further support these observations, we decided to perform experiments in which β-catenin activity was stimulated using BIO, a known inhibitor of GSK3β. Unfortunately, the presence of a constitutive active allele of β-catenin prevented further activation of WNT signalling in H295R cells (data not shown). We thus made use of mouse Y1 adrenocortical cells that express a wild-type version of β-catenin but do not produce aldosterone. As expected, treatment with BIO induced a time-dependent increase in *Axin2* transcription (Supplementary Material, Fig. S3K andL), β-catenin accumulation (Supplementary Material, Fig. S3M) and TOP-FLASH activity in transient transfection experiments (Supplementary Material, Fig. S3N). This was associated with a significant increase in *Cyp11b2* and *Cyp21* expression after 3 and 6 h of treatment (Fig. 3J and K). Increased expression of *Cyp11b2* (Fig. 3L) and *Cyp21* (Fig. 3M) was also observed in the adrenals of 10-month-old ΔCat mice, our model of constitutive β-catenin activation (19). Although we could not detect *At1r* expression in Y1 cells even in the presence of BIO, we observed overexpression of both murine isoforms of *At1r* (*At1a* and *At1b*) in ΔCat adrenals (Fig. 3N). Altogether, these data showed that β-catenin controlled aldosterone production by stimulating the expression of three actors that play an essential role in its synthesis.

β-Catenin controls CYP11B2 expression indirectly

CYP11B2 is the terminal and one of the rate-limiting enzymes for aldosterone synthesis. β-Catenin mostly acts as a transcription coactivator by interacting with transcription factors such as LEF/TCF. We thus evaluated the possibility that β-catenin-controlled *CYP11B2* expression at the transcriptional level. For this, Y1 cells were treated with BIO in the presence or absence of actinomycin D, an inhibitor of transcription. RTqPCR analysis showed that induction of *Cyp11b2* expression by BIO was completely abrogated by actinomycin D, suggesting that β-catenin stimulated the transcription of *Cyp11b2* (Fig. 4A). Computer-assisted analysis of human *CYP11B2* regulatory regions identified two putative LEF/TCF-binding sites at −768/−774 and −1266/−1273 (Fig. 4B; Supplementary Material, Fig. S4). To assess the role of these putative sites in *CYP11B2* promoter activity, we transfected wild-type or mutated constructs of *CYP11B2* regulatory regions in H295R cells (Fig. 4B). As previously published (28), the wild-type promoter drove luciferase expression in H295R cells and strongly responded to Angiotensin II stimulation (Fig. 4C, WT). Surprisingly, mutation of both putative LEF1-binding sites (Fig. 4B) had no effect on basal promoter activity or on Angiotensin II responsiveness (Fig. 4C, Lef mut), suggesting that β-catenin was not acting on *CYP11B2* promoter regions through interaction with LEF/TCF-binding sites. The nuclear receptors NURR1 (NR4A2) and NUR77 (NR4A1) are essential regulators of *CYP11B2* expression in the adrenal (28). We thus evaluated the effect of the three previously published NUR-binding sites on *CYP11B2* promoter activity and on its ability to respond to β-catenin. Treatment of H295R cells with the WNT antagonist PKF115-584 inhibited both basal and Angiotensin II-induced *CYP11B2* promoter activity, confirming that the effect of β-catenin on CYP11B2 expression was essentially transcriptional (Fig. 4D, WT). Mutation of the three NUR-binding sites (NBRE, Ad1, Ad5, Fig. 4B) led to decreased but still measurable levels of promoter activity (Fig. 4D, NBRE/Ad mut). This mutation abrogated promoter response to Angiotensin II and interestingly, it also prevented PKF115-584-mediated repression of promoter activity (Fig. 4D, NBRE/Ad mut). This suggested that the effect of β-catenin on *CYP11B2* regulatory regions was mediated by nuclear receptors of the NUR family.

We initially hypothesized that β-catenin could work as a coactivator of NUR transcriptional activity. However, our repeated transfection experiments failed to provide support for such a theory (data not shown). Therefore, we hypothesized a role of β-catenin in controlling expression of NURs. Indeed, β-catenin knockdown resulted in a significant decrease in *NURR1* (Fig. 5A) and *NUR77* (Fig. 5B) basal and Angiotensin II-induced expression at the mRNA (Fig. 5A and B) and protein level (Fig. 5A and B; Supplementary Material, Fig. S3O and P) in H295R cells. This decrease was also observed in response to PKF115-584 treatment (Supplementary Material, Fig. S3Q and R). Conversely, expression of both nuclear receptors was significantly induced by BIO in Y1 cells (Fig. 5C and D). In agreement with these *in vitro* data, mRNAs for *Nurr1* (Fig. 5E) and *Nur77* (Fig. 5F) were markedly accumulated in 10-month-old ΔCat adrenals. This was further supported by increased expression of *NURR1* in APA compared with NAPA (Fig. 5G). To further analyse the mechanism involving β-catenin in NUR induction, we treated Y1 cells with both BIO and actinomycin D. Actinomycin D abrogated induction of *Nurr1* and *Nur77* mRNA accumulation by BIO (Fig. 5I and J), suggesting that β-catenin acted by stimulating transcription from *Nurr1* and *Nur77* promoters. Sequence analysis of *NURR1* regulatory regions identified two putative Lef/Tcf-binding sites at −57/−61 and +67/+71 that were conserved in mouse and human (Supplementary Material, Fig. S5). Such binding sites were not identified in *NUR77* regulatory regions. However, a recent publication showed that β-catenin could stimulate human *NUR77* expression *in vitro* by associating with c-Jun/c-Fos proteins at four AP1-binding sites (−3/+4, −26/−32, −169/−175 and −189/−195) that were conserved in mouse and human (29) (Supplementary Material, Fig. S6). To confirm binding of β-catenin to these regulatory regions, we performed chromatin immunoprecipitation (ChIP) experiments in H295R cells. β-Catenin bound to both *NURR1* (through LEF/TCF sites) and *NUR77* (through AP1 sites) promoters in untreated cells (Fig. 5K and L). Consistent with our expression analysis data, binding of β-catenin was markedly diminished after incubation with PKF115-584 (Fig. 5K and L). To further confirm these observations, we performed similar ChIP experiments with whole adrenal glands from wild-type or ΔCat mice that overexpress both *Nurr1* and *Nur77* (Fig. 5M and N). Binding of β-catenin to Lef/Tcf or Ap1 sites was almost undetectable in wild-type adrenals. However, it was markedly increased in ΔCat adrenals, in which β-catenin was constitutively activated (Fig. 5M and N). Altogether, these experiments showed that β-catenin could control expression of both nuclear receptors *in vitro* and *in vivo*. It further suggested that the effect of β-catenin on *CYP11B2* expression could be mediated by NURR1 and NUR77. To confirm this hypothesis, NUR binding to *CYP11B2* promoter regions was analysed by *in vitro* and *in vivo* ChIP experiments. In H295R cells, NURR1 and NUR77 bound to the proximal Ad1 and Ad5 sequences (Fig. 5O, top panel) and to a lesser extent to the distal NBRE sequence (Fig. 5O, bottom panel). In both cases, NUR binding was inhibited by the Wnt inhibitor PKF115-584 (Fig. 5O). Although the NUR response elements previously

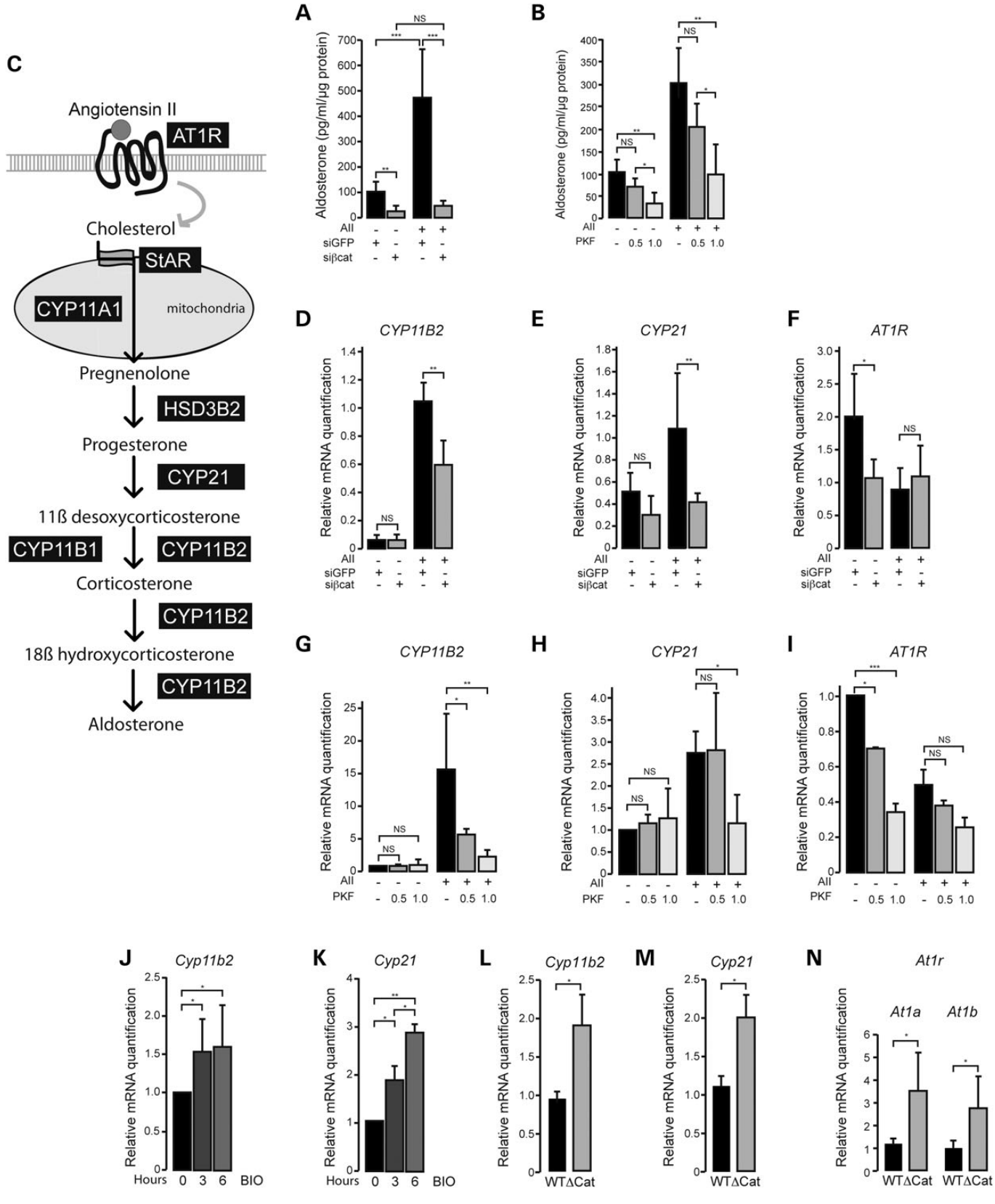

Figure 3. Wnt/β-catenin pathway controls aldosterone secretion. (**A**) β-Catenin knockdown decreases aldosterone secretion. Basal and Angiotensin II-induced aldosterone concentrations were measured on the culture medium from H295R cells that were either transfected with a control siRNA (siGFP) or transfected with a siRNA to β-catenin (siβcat) for 5 days and treated 6 h before harvesting with or without 10 nM Angiotensin II. (**B**) Inhibition of the transcriptional activity of β-catenin decreases aldosterone secretion. Aldosterone concentrations were measured in the medium of H295R cells that were pre-treated for 24 h with DMSO

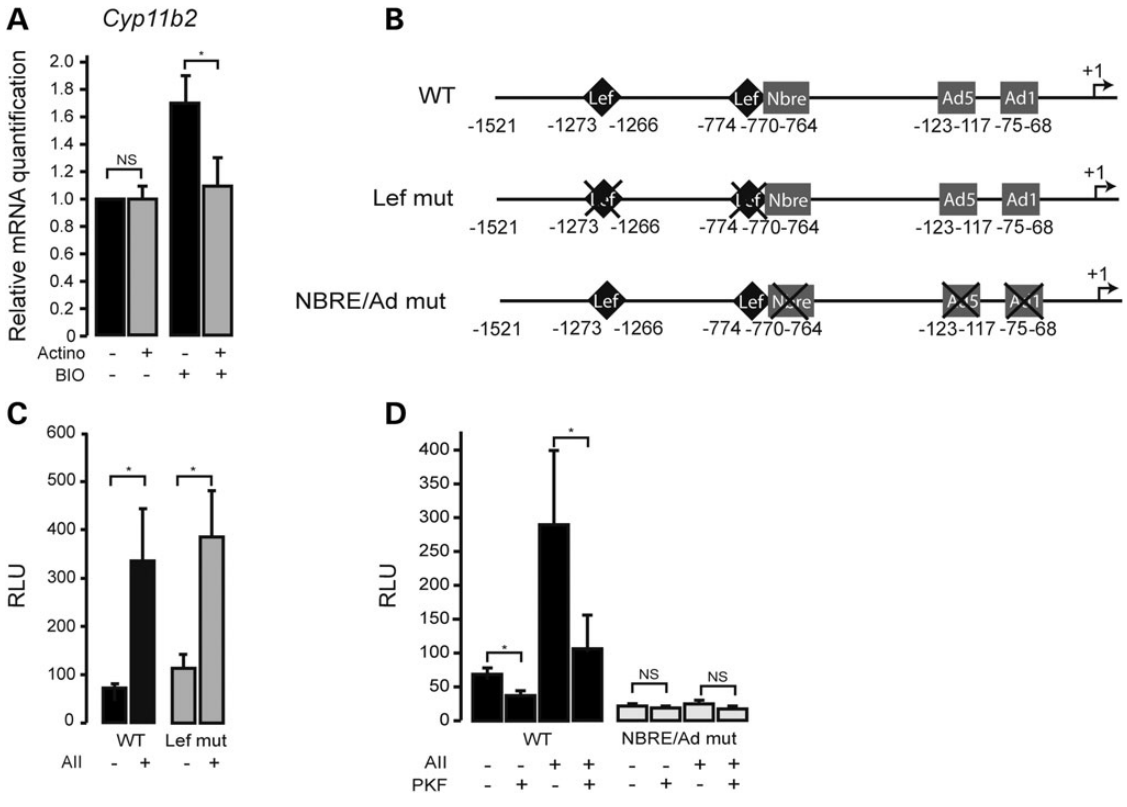

Figure 4. β-Catenin regulates transcription of *CYP11B2* independently of LEF/TCF-binding sites. (**A**) Wnt/β-catenin activation induces transcription of *Cyp11b2*. *Cyp11b2* expression was analysed by RTqPCR on mRNAs from Y1 cells stimulated by DMSO (control group) or 500 nM BIO alone or in combination with 100 nM actinomycin D (transcription inhibitor) for 6 h before harvesting. (**B**) Schematic representation of human *CYP11B2* promoter. WT plasmid encompasses 1521 bp of wild-type human *CYP11B2* promoter regions upstream of the luciferase reporter gene (WT). In Lef Mut plasmid two putative LEF/TCF sites (−768/−774, −1266/−1273) predicted by *in silico* analysis were mutated. In the NBRE/Ad mut plasmid, one NBRE (−764/−770) and two Ad sites (−68/−75, −117/−123) that were previously shown to bind NGF1B nuclear receptors were mutated. (**C**) Mutagenesis of LEF/TCF sites does not alter CYP11B2 basal and Angiotensin II-stimulated promoter activity. H295R cells were transfected for 24 h with WT or Lef mut plasmid and stimulated for 6 h with 10 nM Angiotensin II before relative luciferase activity (RLU) was quantified in protein extracts. Bars represent the mean relative quantification of at least 3 individual experiments ± standard deviation. (**D**) Mutagenesis of NBRE and Ad sites abolishes *CYP11B2* induction by Angiotensin II and prevents repression by PKF-115-584. Relative luciferase activity (RLU) was measured in H295R cells transfected with WT or NBRE/Ad mut plasmids for 16 h. They were then pre-treated for 24 h with DMSO (control group) or 1.0 μM PKF115-584 and treated for 6 h with either 1.0 μM PKF115-584 or 10 nM Angiotensin II alone or a combination of both. Bars in (A) represent the mean relative quantification of at least four individual experiments performed in triplicate ± standard deviation. Bars in (C) and (D) represent the mean RLU value of at least three individual experiments performed in triplicate ± standard deviation. Statistical analyses were performed by one-way ANOVA, followed by Tukey's *post hoc* test. $^{*}P < 0.05$; NS, not significant.

described in human *CYP11B2* regulatory regions were not strictly conserved in mouse *Cyp11b2* regulatory regions, sequence analysis identified a putative Sf-1 response element (+156/+162, also known to bind Nur proteins) downstream of the TSS (transcription start site) and two potential nuclear receptor-binding sites (−174/−150, −233/−247) upstream of the TSS (Supplementary Material, Fig. S4). *In vivo* ChIP experiments showed mild binding of both Nurr1 and Nur77 to the proximal

(control group), 0.5 or 1.0 μM PKF115-584 (Wnt/β-catenin inhibitor) followed by Angiotensin II stimulation alone or in combination with PKF115-584 for 6 h before harvesting. (**C**) Schematic representation of aldosterone biosynthesis pathway. AT1R, Angiotensin II Type 1 Receptor; StAR, steroidogenic acute regulatory; CYP11A1, cytochrome P450 cholesterol side chain cleavage; HSD3B2, 3β-hydroxysteroid dehydrogenase type 2; CYP21, cytochrome P450 21-hydroxylase; CYP11B1, cytochrome P450 11β-hydroxylase; CYP11B2, cytochrome P450 aldosterone synthase. (**D**–**F**) β-Catenin knockdown decreases basal *AT1R* expression and Angiotensin II-induced *CYP11B2* and *CYP21* expression. *AT1R*, *CYP21* and *CYP11B2* expression levels were analysed by RTqPCR on mRNAs from H295R cells transfected with a control siRNA (siGFP) or a siRNA to β-catenin (siβcat) in basal condition or after 6 h 10 nM Angiotensin II treatment. (**G**–**I**) Inhibition of the transcriptional activity of β-catenin down-regulates *CYP11B2*, *CYP21* and *AT1R* expression. *AT1R*, *CYP21* and *CYP11B2* expression levels were analysed by RTqPCR on mRNA from H295R cells that were pre-treated for 24 h with DMSO (control group), 0.5 or 1.0 μM PKF115-584 followed by 10 nM Angiotensin II stimulation alone or in combination with PKF115-584 for 6 h, before harvesting. (**J** and **K**) *Cyp11b2* and *Cyp21* are up-regulated by activation of the Wnt/β-catenin pathway. *Cyp11b2* and *Cyp21* expression levels were analysed by RTqPCR on mRNAs from the mouse Y1 adrenocortical cells that were induced with DMSO (control group) or 500 nM of BIO, an activator of Wnt/β-catenin signalling for 3 or 6 h. (**L**–**N**) *Cyp11b2*, *Cyp21* and *At1r* expression levels are increased in the adrenals of mice with constitutive β-catenin activation. Expression of *Cyp11b2*, *Cyp21* and the two mouse *At1r* genes (*At1a* and *At1b*) was analysed by RTqPCR on mRNAs extracted from 10-month-old wild-type ($n = 6$) and ΔCat ($n = 6$) mice. Bars in (A) and (B) represent the mean aldosterone concentration in culture medium (normalized to protein content) from at least four individual experiments performed in triplicate ± standard deviation. Bars in (D)–(K) represent the mean quantification of at least four individual experiments performed in triplicate ± standard deviation. Bars in (L)–(N) represent the mean relative quantification ($n = 6$) ± standard deviation. Statistical analyses in (A)–(K) were performed by one-way ANOVA followed by Tukey's *post hoc* test. Statistical analyses in (L)–(N) were conducted by Student's *t*-test. $^{*}P < 0.05$; $^{**}P < 0.005$; NS, not significant.

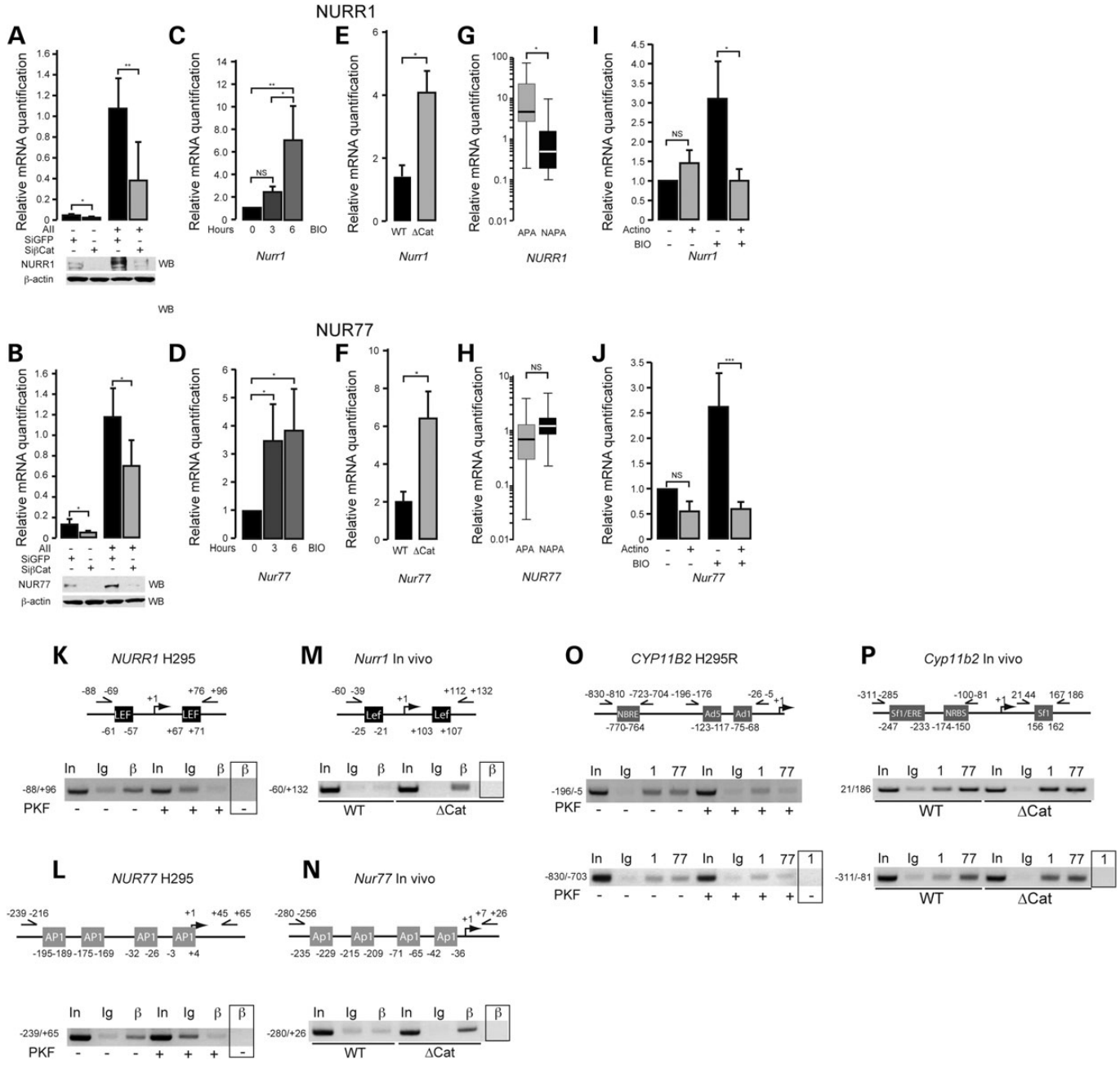

Figure 5. β-Catenin controls *CYP11B2* transcription through stimulation of *NGFIB* nuclear receptors expression (**A** and **B**) β-catenin knockdown decreases *NURR1* and *NUR77* expression. *NURR1* and *NUR77* expression levels were analysed by RTqPCR on mRNAs and by western blot on proteins extracts (bottom panels) from H295R transfected for 5 days with control siRNA (siGFP) or a siRNA to β-catenin (siβcat) and treated for 6 h with 10 nM Angiotensin II. (**C** and **D**) Wnt/β-catenin activation induces *Nurr1* and *Nur77* expression. *Nurr1* and *Nur77* expression levels were analysed by RTqPCR on mRNA from Y1 cells that were treated with DMSO (control group) or 500 nM of BIO for 3 or 6 h. (**E** and **F**) *Nurr1* and *Nur77* expression levels are increased in the adrenals of mice with constitutive β-catenin activation. Expression of *Nurr1 and Nur77* was analysed by RTqPCR on mRNAs extracted from 10-month-old wild-type ($n = 6$) and ΔCat ($n = 6$) mice. (**G** and **H**) *NURR1* expression is up-regulated in APA. *NURR1* and *NUR77* expression levels were analysed by RTqPCR on mRNAs from 35 APA and 17 NAPA. (**I** and **J**) β-Catenin stimulates transcription of *Nurr1* and *Nur77. Nurr1* and *Nur77* expression levels were analysed by RTqPCR on mRNAs from Y1 cells stimulated by DMSO (control group) or 500 nM BIO alone or in combination with 100 nM actinomycin D for 6 h. (**K** and **L**) β-Catenin binding to *NURR1* and *NUR77* regulatory regions is inhibited by PKF115-584 in H295R cells. H295R cells were treated with DMSO (control group) or 1.0 μM PKF115-584 for 30 h. After treatment, cells were fixed and sheared chromatin was immunoprecipitated with 5 μg of a control immunoglobulin (Ig) or 5 μg of an antibody to β-catenin (β). PCRs were performed with primers (arrows) flanking two conserved putative LEF/TCF-binding sites in *NURR1* regulatory regions (K) and four previously described AP1-binding sites in *NUR77* promoter (L). Boxed lanes represent control immunoprecipitation experiments performed with β-catenin antibody and primers located in the coding sequences of *NURR1* and *NUR77*. (**M** and **N**) β-Catenin binding to *Nurr1* and *Nur77* regulatory regions is increased in adrenals from ΔCat mice. Adrenals from six wild-type and six ΔCat mice were fixed and the sheared chromatin was immunoprecipitated with control (Ig) or β-catenin (β) antibodies. PCRs were performed with primers flanking two conserved putative Lef/Tcf-binding sites in *Nurr1* regulatory regions (M) and four conserved Ap1-binding sites in *Nur77* promoter (N). Boxed lanes represent control immunoprecipitation experiments performed with β-catenin antibody and primers located in the coding sequences of *Nurr1* and *Nur77*. Positions in the four cartoons are relative to the transcription start site. (**O**) NURR1 and NUR77 binding to *CYP11B2* regulatory regions are inhibited by

Sf-1 response element region in wild-type adrenals extracts (Fig. 5P, top panel). It also showed binding of Nur77 and to a lesser extent of Nurr1 to the distal sites (Fig. 5P, bottom panel). Binding of Nurr1 to the proximal Sf-1 response region was increased in ΔCat adrenals (Fig. 5P). There was also a mild increase in Nurr1 binding to the distal element, whereas Nur77 binding was not altered in ΔCat adrenals (Fig. 5P). Collectively, these data strongly suggested that β-catenin controlled *CYP11B2* expression indirectly, through stimulation of *NURR1* and *NUR77* transcription.

Control of *CYP21* and *AT1R* expression involves direct and indirect mechanisms

We then addressed the mechanisms of CYP21 regulation. As for *Cyp11b2*, induction by BIO in Y1 cells was abrogated by incubation with actinomycin D, suggesting that the effect of β-catenin on *Cyp21* expression was transcriptional (Fig. 6A). Computer-assisted promoter analysis identified one putative LEF/TCF-binding site (−82/−86) and two putative NUR response elements (−130/−135, −62/−67) upstream of the TSS in both human and mouse *CYP21* (Supplementary Material, Fig. S7). ChIP analysis in H295R cells showed binding of both β-catenin (Fig. 6B, top panel) and NURR1/NUR77 (Fig. 6B, bottom panel) to this promoter region. Binding of these three transcriptional activators was disrupted by PKF115-584 (Fig. 6B). This suggested that β-catenin could control expression of *CYP21* both directly (by interacting with LEF/TCF factors) and indirectly by stimulating NUR expression. Sequence analysis of mouse *Cyp21* regulatory regions identified four non-conserved distal (−629/−632, −623/−627, −608/−612, −370/−374) and three proximal putative Lef/Tcf-binding sites (−142/−146, −53/−57, −34/−30) as well as one putative Sf-1 (−280/−285) and four putative proximal Nur-binding sites (−189/−194, −122/−127, −49/−55, −4/−8) (Supplementary Material, Fig. S7). In wild-type mice, β-catenin binding was almost undetectable, whereas Nurr1 and Nur77 bound to the distal (Fig. 6C, top panel) and to a lesser extent to the proximal regions (Fig. 6C, bottom panel). Binding of β-catenin and *Nurr1* to the distal and proximal regions was markedly increased in ΔCat mice compared with wild-type mice (Fig. 6C). Altogether, these experiments suggested that *CYP21* was both a direct and indirect target of β-catenin in human adrenocortical cells and in mouse adrenals *in vivo*.

We finally addressed the regulation of *AT1R* expression by β-catenin. *In silico* analysis of *AT1R* regulatory regions showed one putative LEF/TCF-binding site on human *AT1R* promoter. This site was conserved in mouse *At1a* regulatory regions (Supplementary Material, Fig. S8), but not in mouse *At1b* promoter, which harbored one putative Ap1-binding site (Supplementary Material, Fig. S9). ChIP analysis showed binding of β-catenin in a region surrounding the putative LEF-binding site (−502/−505) on human *AT1R* promoter in H295R cells. As expected, binding was markedly diminished by PKF115-584 treatment (Fig. 6D). In mouse adrenals, ChIP analysis showed binding of β-catenin to the regions surrounding the putative Lef- and Ap1-binding sites on *At1a* and *At1b* promoters, respectively (Fig. 6E). This was markedly increased in ΔCat, compared with wild-type adrenals (Fig. 6E). This strongly suggested that β-catenin could directly control expression of *AT1R* and *At1a*/*At1b* in human and mouse adrenocortical cells, respectively.

DISCUSSION

Our study provides strong immunohistochemical and molecular evidence that WNT/β-catenin signalling is aberrantly activated in 70% of APA in a series of 47 patients, which is the most frequent molecular alteration reported in APA, to our knowledge. The observation that mice with adrenal-specific constitutive activation of β-catenin displayed increased aldosterone production suggested that aberrant WNT signalling may be driving the development of APA (19). Here, using a combination of *in vitro* and *in vivo* experiments, we show that β-catenin is essential for both basal and Angiotensin II-induced aldosterone production. We further show that this function of β-catenin relies on its transcriptional activity, which stimulates expression of three major actors of aldosterone synthesis, i.e. *AT1R*, *CYP21* and *CYP11B2*, through direct and indirect mechanisms involving NURR1 and NUR77 (Fig. 7). Finally, we show that there is no obvious association between *KCNJ5* mutations and activation of WNT signalling, suggesting that the two pathways act independently in APA and may promote formation of different types of tumours. Altogether, these data strongly suggest that abnormal WNT pathway activation is closely associated with the development of PA in patients.

In the adrenal gland, constitutive WNT/β-catenin signalling has already been involved in the development of NAPA, micro- and macronodular hyperplasia and adrenocortical carcinomas (reviewed in 20). In most cases, increased activation, as assessed by immunohistochemistry or gene expression array analysis, was correlated with more aggressive disease (30–33). That WNT/β-catenin signalling plays a central role in the establishment of

PKF115-584. H295R cells were treated as described above and sheared chromatin was immunoprecipitated with 5 μg of a control Ig, 5 μg of an antibody to NURR1 (1) or 5 μg of an antibody to NUR77 (77). PCRs were performed with one set of downstream primers flanking Ad1 and Ad5 sequences (top panel) and one set of upstream primers flanking the NBRE sequence (bottom panel). Boxed lane represents a control immunoprecipitation experiment performed with NURR1 antibody and primers located in the coding sequence of *CYP11B2*. (**P**) Nurr1 binding to mouse *Cyp11b2* regulatory regions is increased in adrenals from ΔCat mice. Adrenals from six wild-type and 6 ΔCat mice were fixed and the sheared chromatin was immunoprecipitated with 5 μg of a control immunoglobulin (Ig), 5 μg of an antibody to Nurr1 (1) or 5 μg of an antibody to Nur77 (77). PCRs were performed with one set of downstream primers flanking a putative Sf-1-binding site (top panel) and one set of upstream primers flanking putative Sf-1 and nuclear receptors binding sites (NRBS, bottom panel). Boxed lane represents a control immunoprecipitation experiment performed with NURR1 antibody and primers located in the coding sequence of *Cyp11b2*. Positions in the two cartoons are relative to the transcription start site. All ChIP experiments were repeated at least three times. 'In' refers to 10% of the amount of chromatin that was loaded in each immunoprecipitation and serves as a reference (10% input). Bars in (A)–(D) and (I) and (J) represent the mean relative quantification of at least four individual experiments performed in triplicate ± standard deviation. Bars in (E) and (F) represent the mean relative quantification ($n = 6$) ± standard deviation. Statistical analyses in (A)–(D) and (I) and (J) were performed by one-way ANOVA followed by Tukey's *post hoc* test. Statistical analyses in (E) and (F) were conducted by Student's *t*-test. Statistical analyses in (G) and (H) were conducted by Welch's *t*-test to account for different variances. $^{*}P < 0.05$; $^{**}P < 0.005$; $^{***}P < 0.0005$; NS, not significant.

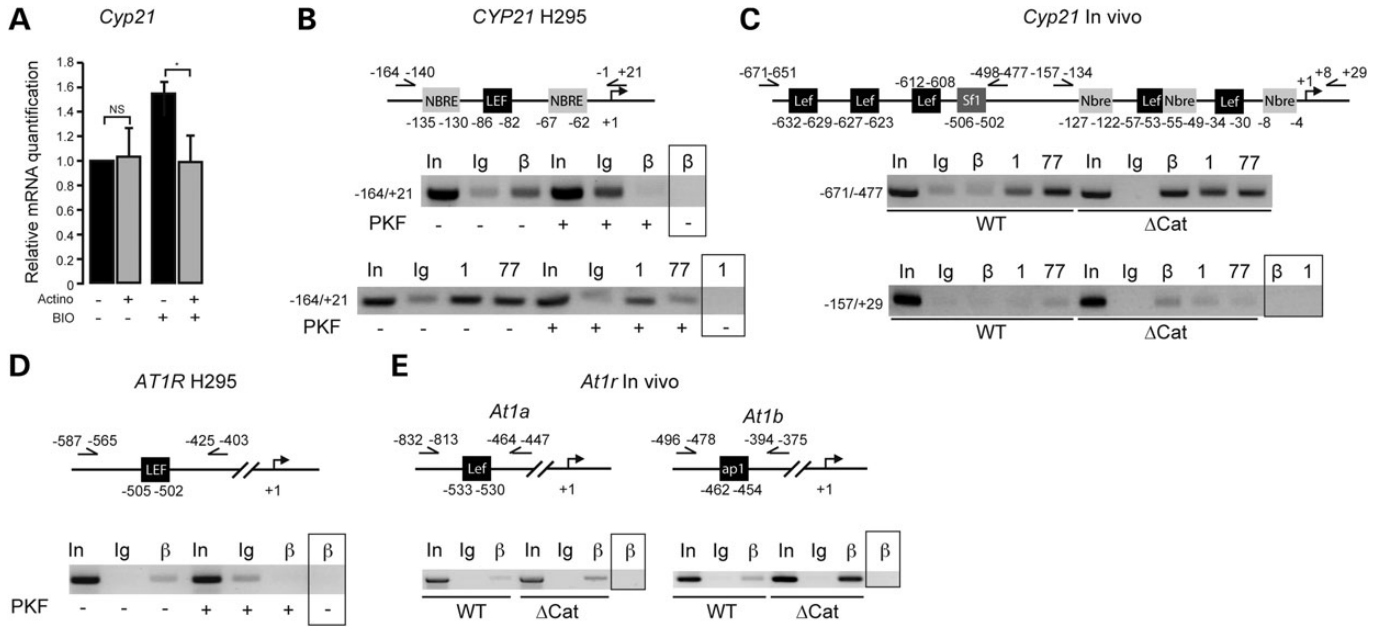

Figure 6. β-Catenin stimulates *CYP21* and *AT1R* expression. (**A**) β-Catenin induces transcription of *Cyp21*. *Cyp21* expression was analysed by RTqPCR on mRNAs from Y1 cells stimulated by DMSO (control group) or 500 nM BIO alone or in combination with 100 nM actinomycin D for 6 h. Bars represent the mean relative quantification of at least four individual experiments performed in triplicate ± standard deviation. (**B**) β-Catenin and NURs binding to *CYP21* promoter is inhibited by PKF115-584. H295R cells were treated as described in Figure 5 and sheared chromatin was immunoprecipitated with 5 μg of a control immunoglobulin (Ig), 5 μg of an antibody to β-catenin (β, top panel), 5 μg of an antibody to NURR1 (1, bottom panel) or 5 μg of an antibody to NUR77 (77, bottom panel). PCRs were performed with primers flanking one putative LEF/TCF-binding site and one NBRE. Boxed lanes represent control immunoprecipitation experiments performed with β-catenin and NURR1 antibodies and primers located in the coding sequence of *CYP21*. (**C**) β-Catenin and Nurr1 binding to mouse *Cyp21* promoter is increased in ΔCat adrenals. Adrenals from six wild-type and six ΔCat mice were fixed and the sheared chromatin was immunoprecipitated with 5 μg of a control immunoglobulin (Ig), 5 μg of an antibody to β-catenin (β), 5 μg of an antibody to Nurr1 (1) or 5 μg of an antibody to Nur77 (77). PCRs were performed with one set of upstream primers flanking a combination of putative Lef/Tcf, Nbre and Sf-1-binding sites (top panel) and one set of downstream primers flanking putative Lef/Tcf and Nbre-binding sites (bottom panel). Boxed lanes represent control immunoprecipitation experiments performed with β-catenin and NURR1 antibodies and primers located in the coding sequence of *Cyp21*. (**D**) β-Catenin binding to *AT1R* promoter is inhibited by PKF115-584. H295R cells were treated as described above and sheared chromatin was immunoprecipitated with 5 μg of a control immunoglobulin (Ig) or 5 μg of an antibody to β-catenin (β). PCRs were performed with primers flanking one putative LEF/TCF-binding site. Boxed lane represents a control immunoprecipitation experiment performed with β-catenin antibody and primers located in the coding sequence of *AT1R*. (**E**) β-Catenin binding to *At1a* and *At1b* promoters is increased in ΔCat adrenals. Adrenals from six wild-type and six ΔCat mice were fixed and the sheared chromatin was immunoprecipitated with 5 μg of a control immunoglobulin (Ig), or 5 μg of an antibody to β-catenin. PCRs were performed with one set of primers flanking a putative Lef1-binding site in *At1a* promoter (left panel) and one set of primers flanking one putative Ap1 site in *At1b* promoter (right panel). Positions in the three cartoons are relative to the transcription start site. Boxed lanes represent control immunoprecipitation experiments performed with β-catenin antibodies and primers located in the coding sequences of *At1a* and *At1b*. All ChIP experiments were repeated at least three times. 'In' refers to 10% of the amount of chromatin that was loaded in each immunoprecipitation and serves as a reference (10% input). Statistical analysis in (A) was performed by one-way ANOVA followed by Tukey's *post hoc* test. $^*P < 0.05$; NS, not significant.

APA, in essence a benign adrenal tumour thus seems puzzling. However, one essential aspect of WNT signalling is its high sensitivity to dosage, which is essential for A–P axis and organ patterning. This is also reflected in different dosage requirements for tumourigenesis in transgenic mouse models (34–38). In our previously published mouse model of constitutive β-catenin activation (19), although a good number of cells with accumulation of β-catenin displayed Cyp11b2 expression, cells with highest levels of accumulation were rather undifferentiated Fig. 5 in reference 19. Furthermore, the most aggressive tumours in ΔCat mice did not overproduce aldosterone (19) (Supplementary Material, Fig. S4 in reference 19). This suggests that levels of WNT dosage may also play a central role in the development of specific types of tumours within the adrenal cortex.

The mechanisms involved in WNT pathway activation in non-aldosterone secreting adrenal tumours are not completely understood. However, 36% of adrenocortical adenomas (usually the largest ones) and 16% of carcinomas (usually the most aggressive ones) display activating mutations of the CTNNB1 gene (30,31,32). In contrast, our analysis of *CTNNB1* gene sequence failed to identify any activating mutations in APA, which was in line with previously published data (21). It is therefore possible that the levels of WNT pathway activation achieved in APA differ quite significantly from the levels found in other adrenal tumours. Here, using transcriptome and RTqPCR analyses, we show down-regulation of the secreted WNT inhibitor *SFRP2* (39), which is significantly inversely correlated with *AXIN2* and *CYP11B2* expression. We also demonstrate for the first time that *Sfrp2* knockout mice have significantly increased plasma aldosterone levels that are significantly correlated with increased *Axin2* expression, abnormal β-catenin accumulation and marked adrenal dysplasia. Although it is quite likely that other factors play a role in WNT pathway activation in APA, our data strongly suggest that decreased SFRP2 expression contributes to the establishment of a particular dosage of WNT signalling, which is associated with the development of APA. In light of these observations, it will be interesting to evaluate expression of WNT pathway regulators in other types of adrenal tumours, in correlation with WNT signalling activity.

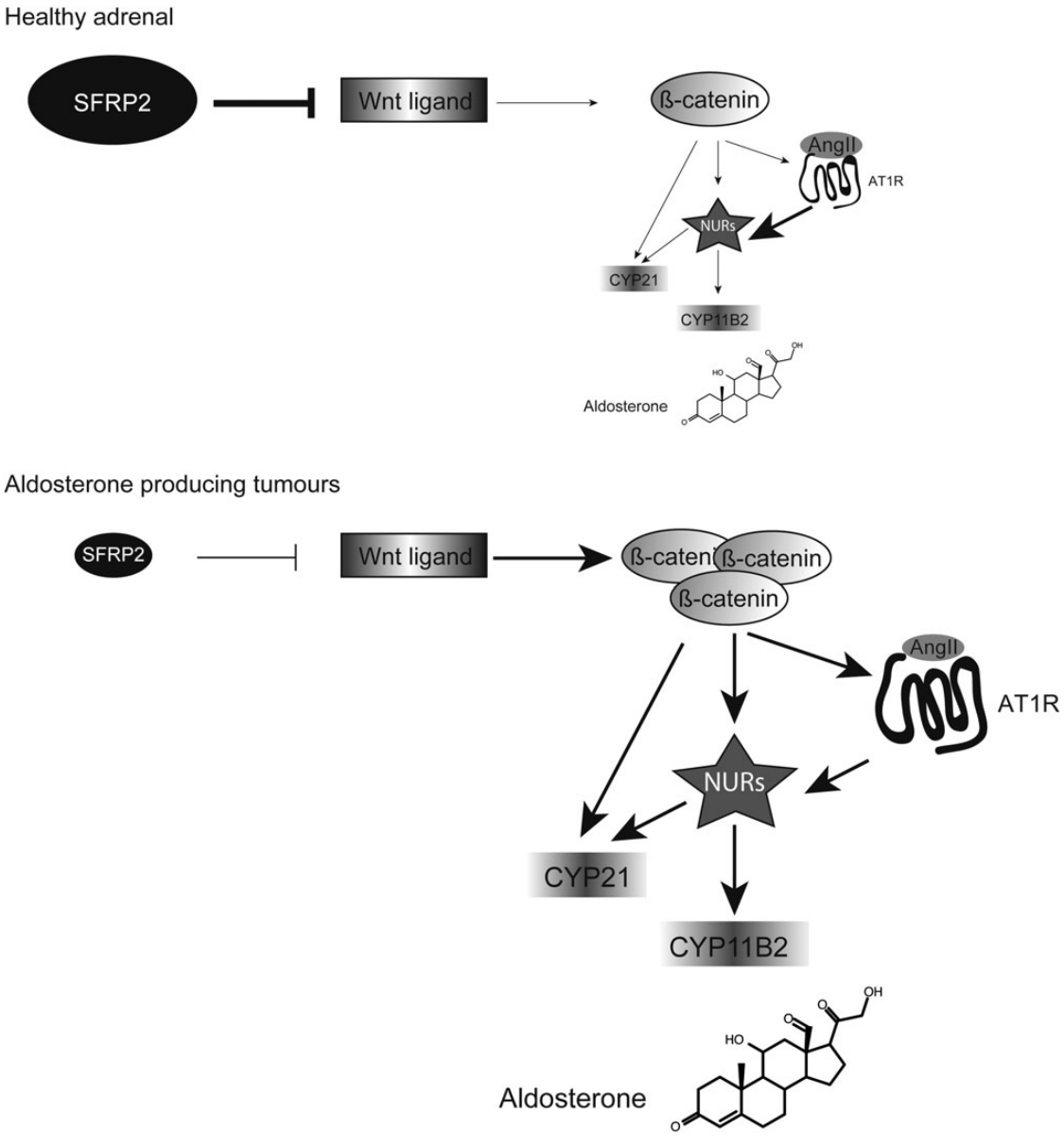

Figure 7. Synthetic representation of the main findings of this study. In a healthy adrenal (top panel), WNT signalling is maintained at a basal level by the action of SFRP2 (and presumably other actors of WNT signalling). Aldosterone secretion is stimulated by Angiotensin II through a cascade involving binding of Angiotensin II to its receptor AT1R, which stimulates NURR1 and NUR77 (NURs) expression. These in turn control the expression of CYP21 and CYP11B2, two enzymes essential for aldosterone production. Whether β-catenin plays a role in the control of aldosterone production in a healthy adrenal is unknown. In aldosterone-producing tumours (bottom panel), down-regulation of SFRP2 (or other regulators) results in deregulated WNT/β-catenin activation (70% of APA). β-Catenin is constitutively bound to the promoters of *AT1R*, *NURR1* and *NUR77*. This results in increased expression of these genes, which in turn stimulates expression of *CYP21* and *CYP11B2*, leading to increased production of aldosterone.

SFRP2 expression is decreased in a number of tumour types where it correlates with increased WNT signalling. In most tumours, down-regulation of *SFRP2* expression is the result of increased promoter DNA methylation (23,40,41). Although we cannot rule out increased methylation in a subset of cells within APA tissues, our global methylation analyses using pyrosequencing do not show an overall increase in the methylation status of *SFRP2* regulatory regions (Supplementary Material, Fig. S10). This suggests involvement of some other molecular mechanisms. Interestingly, micro-RNAs miR-218 (42), miR-29 (43), miR-410, miR-433 (44) and miR-224 (45) have been proposed as regulators of *SFRP2* expression and WNT signalling. It is therefore tempting to speculate that overexpression of some of these micro-RNAs could account for decreased *SFRP2* expression in APA.

Our observations raise the question of the role of WNT signalling in zona-glomerulosa physiology. Active β-catenin, identified by nucleo-cytoplasmic staining in immunohistochemistry is found mostly restricted to the adrenal zona glomerulosa in wild-type mice (19,46) and in healthy subjects (21), which suggests that WNT pathway is normally activated in this specific zone. Unfortunately, mice with Sf-1:Cre-mediated ablation of

β-catenin exhibit adrenal aplasia in late development, which precludes analysis of postnatal adrenal function (46). Interestingly, however, *Wnt4* knockout mice have impaired zona-glomerulosa differentiation and lower plasma aldosterone concentration at birth. This effect is zone specific as *Cyp21a1* expression and corticosterone levels are not altered (47). Conversely, overexpression of WNT4 in human adrenocortical cell lines increases *CYP11B2* expression and aldosterone production (48). This strongly suggests that WNT4 may be essential to establish a normal pattern of β-catenin activation in adrenal zona glomerulosa. On the basis of our data, we can speculate that this pattern of activation could be involved in the establishment of zona-glomerulosa identity through stimulation of *AT1R* and *CYP11B2* expression. Interestingly, our experiments show that β-catenin knockdown not only decreases aldosterone production but also robustly stimulates CYP17 expression (Supplementary Material, Fig. S11A) and DHEA (Supplementary Material, Fig. S11B) production at the expense of cortisol (Supplementary Material, Fig. S11C) in H295R cells. Although cell culture experiments are to be considered with caution, this suggests that alterations in WNT signalling pathway activity and β-catenin dosage can result in a switch from one hormonal production phenotype to another. It is therefore tempting to speculate that localized WNT signalling pathway activation plays an essential role in the establishment of functional adrenal zonation through both promotion of zona glomerulosa and inhibition of zona fasciculata/reticularis differentiation. Future experiments aiming at inactivating *Ctnnb1* specifically in zona-glomerulosa or fasciculata cells should clarify these hypotheses.

β-Catenin is involved in the control of steroidogenesis in the ovary, where its activity relies on physical and functional interactions with the nuclear receptor SF-1 on *StAR* and *CYP19A1* promoter (49–53). In contrast, we have shown that β-catenin controls adrenal expression of *CYP21* and *CYP11B2* through a novel molecular mechanism involving stimulation of the transcription of the NGFIB family nuclear receptors, NURR1 and NUR77. NUR77 was previously identified as a target gene of β-catenin in colon cancer lines (29). Here, we extend these findings to the adrenal cortex *in vitro* and *in vivo*. We also show that NURR1, another member of the NGFIB family of nuclear receptors, is a transcriptional target for β-catenin. Interestingly, both NUR77 and NURR1 have been shown to inhibit the activity of β-catenin either by inducing its degradation (54) or by decreasing its activity as a transcriptional coactivator (55). These observations are suggestive of a regulation loop in which β-catenin induces NGFIB family members expression which in turn negatively feedback on the transcriptional activity of β-catenin. Our mechanistic findings are thus likely to extend to a number of tissues such as the pancreas, lung or cervix in which both β-catenin and NGFIB nuclear receptors have been involved in tumourigenesis (56–58).

Treatment of a majority of PA cases relies on mineralocorticoid-receptor antagonists. However, most of the time, these inhibitors do not achieve normalization of blood pressure and are associated with endocrine side effects, which decrease patients' compliance with treatment (4–6). We have conducted a pilot study in which ΔCat mice were fed a control or 0.2% quercetin-enriched diet (Supplementary Material, Fig. S12). After 90 days on the specific diets, mice receiving quercetin showed a significant and specific decrease in aldosterone production (Supplementary Material, Fig. S12A and B), which was correlated with decreased Wnt pathway activity (Supplementary Material, Fig. S12C). Quercetin is the most abundant dietary flavonoid endowed with the capacity to inhibit multiple intracellular signalling pathways, amongst which β-catenin interaction with LEF/TCF (59,60). Interestingly, increased quercetin consumption is associated with a decrease in blood pressure in animal models (61) and in hypertensive patients (62). Although multiple molecular mechanisms have been proposed to account for these activities (62), on the basis of our data, we propose that some of the hypotensive effects of quercetin may be mediated by inhibition of WNT signalling and aldosterone secretion in the adrenal cortex. The broad spectrum of quercetin activities is probably incompatible with clinical use as an inhibitor of WNT signalling. However, small molecule drugs targeting β-catenin are emerging in Phase I and II clinical trials (63). Their therapeutic potential for the treatment of PA remains to be evaluated.

In conclusion, our data provide novel molecular insights that account for a large number of APA in patients. They show that aberrant WNT pathway activation plays a central role in the aetiology of this disease and suggest that it may be a relevant pharmacological target to allow normalization of aldosterone production in patients with APA.

MATERIALS AND METHODS

Ethics statement

Studies on patients' samples were conducted in agreement with the principles of the declaration of Helsinki and were approved by CPP (Comité de Protection des Personnes) Ile de France II. All participants gave informed consent for the study. All animal studies were approved by Auvergne Ethics committee and were conducted in agreement with international standards for animal welfare (protocols CE 76-12 and CE 77-12).

Patients

We obtained formalin-fixed and paraffin-embedded adrenals through the COrtico- et MEdullo-surrénale Tumeurs Endocrines (COMETE) network from 31 patients and 17 patients who had undergone surgery for APA at Hôpital Européen Georges Pompidou and Cochin Hospital, respectively (Plan Hospitalier de Recherche Clinique Grant AOM06179 to the COMETE-INCa network). The clinical and biological characteristics of the patients are summarized in Supplementary Material, Table S1A. Methods for screening and criteria for diagnosing PA and APA were in accordance with institutional guidelines. For controls, we selected 17 secreting NAPA, which were diagnosed in the Endocrinology Department of Cochin Hospital. These did not have nucleocytoplasmic accumulation of β-catenin, which was considered as the criteria for absence of constitutive Wnt pathway activation. Our retrospective transcriptome analyses were performed with the datasets from six APA and four control adrenals of the Cochin/COMETE series that were previously analysed on cDNA microarrays (22). These analyses were carried out using 'R' (http://www.r-project.org/). The LIMMA test was used for group comparisons (LIMMA R package) and *P* values were adjusted using the

Benjamini–Hochberg correction method. All data are available on ArrayExpress web site (http://www.ebi.ac.uk/arrayexpress, experiment E-TABM-311, samples CIT-HS-ACT-EC-ACA17, CIT-HS-ACT-EC-ACA19, CIT-HS-ACT-EC-ACA29, CIT-HS-ACT-EC-ACA39, CIT-HS-ACT-EC-ACA40, CIT-HS-ACT-EC-ACA42, CIT-HS-ACT-EC-NA1, CIT-HS-ACT-EC-NA2, CIT-HS-ACT-EC-NA3, CIT-HS-ACT-EC-NA4). RTq PCR analyses were performed on the same 6 APA and 11 NAPA as well as on 29 additional APA from the HEGP/COMETE series and 6 NAPA from the Cochin/COMETE series (see Supplementary Material, Table S1B). Seven NA were obtained from radical nephrectomies (Cochin/COMETE and Rouen/COMETE). All patients gave written informed consent to participate to the study.

Immunohistochemistry

Immunohistochemistry for β-catenin, Dab2 and Cyp11b2 was performed on tissues embedded in paraffin as previously described (19,26,64). For patients' samples, the entirety of β-catenin-stained sections was examined. Immunohistochemical labelling was evaluated by a trained pathologist for the presence of membrane, cytoplasmic and nuclear staining by a qualitative assessment. The intensity of staining was not scored. Images were acquired with a Zeiss Axioplan 2 microscope and Axiocam HR camera. They were minimally processed for global levels and white balance using Adobe Photoshop®.

In situ hybridization

In situ hybridization analyses for human *CYP11B2* detection were conducted as previously described (21).

Patients' DNA sequencing

For identification of *KCNJ5* mutations, the DNA coding for amino acids 122–199 was sequenced as described in (17). Mutations in the third and fifth exons of *CTNNB1* gene were analysed as described in (21).

Genomic DNA methylation analysis

Methylation analyses were conducted on genomic DNA from 4 NA, 15 NAPA devoid of β-catenin activation and 11 APA (see Supplementary Material, Table S1B). Genomic DNA was extracted from tumour samples using standard procedures and 500 ng of sample DNA were bisulfite treated by EpigenDx (Hopkinton, MA, USA) using a proprietary bisulphite salt solution. Briefly, DNA was diluted to 45 and 5 μl of 3 N NaOH were added, followed by a 30-min incubation at 42°C to denature the DNA. One hundred microliters of bisulfite salt solution were added to the DNA and incubated for 14 h at 50°C. Bisulfite-treated DNA was purified using Zymogen DNA columns and was eluted 20 μl of TE, pH 8.0. One microliter of the converted DNA was used for each PCR reaction. The PCR was performed with 0.2 μM of each primer. One of the PCR primers was biotinylated to purify the final PCR product using Sepharose beads. The PCR product was bound to Streptavidin Sepharose HP (GE Healthcare), and the Sepharose beads containing the immobilized PCR product were purified, washed and denatured using a 0.2-M NaOH solution. They were the washed using the Pyrosequencing Vacuum Prep Tool (Pyrosequencing, Qiagen) as recommended by the manufacturer. Then 0.2 μM pyrosequencing primer was annealed to the purified single-stranded PCR product. Ten microliters of the PCR products were sequenced by Pyrosequencing PSQ96 HS System (Biotage AB) following the manufacturer's instructions (Pyrosequencing, Qiagen). The methylation status of each locus was analysed individually as a T/C SNP using QCpG software (Pyrosequencing, Qiagen). The percentage of methylation at each CpG site was compared between normal adrenal, NAPA and APA using Anova followed by Tukey's *post hoc* test.

Mice

All animal studies were approved by Auvergne Ethics committee and were conducted in agreement with international standards for animal welfare (protocols CE 76-12 and CE 77-12). Sfrp2 mice (on a Sv129EV/C57Bl6 mixed background) were kindly provided by Dr Brendan Lee and were previously described (24). ΔCat mice (on a pure C57Bl6 background) were generated in our lab and were previously characterized (19). Female *Sfrp2* knockout mice were fed a standard diet (SAFE, U8958v106). Blood was collected by retro-orbital puncture in 2 μl EDTA at different time points and used for plasma aldosterone concentration measurement. Individual increases in plasma aldosterone were found as early as 7 months but were only significant in the knockout group at 13 months. After the experiment, mice were euthanized by decapitation and blood was collected on vacuum blood collection tubes (VF-053STK, Terumo). Adrenals were either frozen in liquid nitrogen or fixed in 4% PFA. Ten-month-old female ΔCat mice were fed with either a standard control diet (Safe, A03) or a 0.2% quercetin-enriched diet (based on Safe A03) for 3 months. Blood and tissues were collected and processed as described above. Littermate control animals were used in all experiments.

Cell culture

Human adrenocortical cancer H295R cell line was grown as previously described with DMEM/Ham's F12 supplemented with 10% fetal bovine serum (S1800-500, Biowest), 2 mM L-glutamine (25030, Gibco), 50 U/ml penicillin, 100 μg/ml streptomycin and 1 × insulin transferrin selenium (41400-045, Gibco). Mouse adrenocortical tumour Y1 cell line was grown with DMEM/Ham's F12 supplemented with 10% fetal bovine serum (S1800-500, Biowest), 2 mM L-glutamine (25030, Gibco), 50 U/ml penicillin and 100 μg/ml streptomycin.

Statistical analyses

Statistical analysis of RTqPCR, western-blot and transfection data was performed with GraphPad Prism5 software. When *t*-test was applied, variance was always evaluated. In case of unequal variances, Welch's *t*-test was performed. In all boxplot and scatter plot representations whiskers show the minimum and maximum values for each population. For methylation analyses, outliers are represented as dots detached from the boxplots.

Plasmids

TOP- and FOP-FLASH vectors were a kind gift of Dr Perret (Institut Cochin). Reporter plasmids hCYP11B2 (pB2-1521) WT and NBRE/Ad5/Ad1M were kindly provided by William E. Rainey (Department of Physiology, Medical college of Georgia, Augusta, GA, USA) (28). For the LEF/TCF mutant construct, the two LEF/TCF sequences 5′-CTTTGCTG-3′ (−1266/−1273) and 5′-CTTTGAAAAGG-3′ (−768/−774) were changed to 5′-agggtcgG-3′ and 5′-agggtccAAGG-3′, respectively, using the QuickChange II kit (Stratagene). All bases were numbered relative to hCYP11B2 transcriptional start site.

Cell transfections and treatment

H295R cells were seeded at a density of 8×10^5 cells per well in 6-well plate. The day after seeding, 1 μg of reporter plasmid DNA was transiently transfected using Transfast reagent (Promega) according to manufacturer's instructions. Following transfection, cells were incubated with 2 ml minimum medium for 16 h (DMEM/F12 medium containing L-glutamine and antibiotic). Where indicated, cells were pre-treated for 24-h with 1.0 μM PKF115-584 (WNT/β-catenin inhibitor, El-198-0100, Enzo Life Sciences), followed by 10 nM of Angiotensin II (A9525, Sigma-Aldrich) alone or in combination with PKF115-584 for 6 h. Control cells were treated with DMSO, which was used as the vehicle for PKF115-584. Cells were then lysed in reporter lysis buffer (E3971, Promega) and assayed for luciferase activity with the GenofaxA luciferase assay system (Yelen). All experiments were performed in triplicate and repeated at least thrice.

To evaluate the effect of Wnt pathway inhibition, H295R cells were seeded in 6-well plate at a density of 8×10^5 cells per well plate and cultured in minimum medium overnight before pretreatment for 24-h with 0.5 or 1.0 μM PKF115-584 or DMSO (control group). After this, the cells were treated with 10 nM of Angiotensin II alone or in combination with PKF115-584 for 6 h.

For knockdown experiments, siRNA sequences targeting β-catenin 5′-AGCUGAUAUUGAUGGACAG-3′ and GFP 5′-ACUACCAGCAGAACACCCCUU-3′ were used. H295R cells were seeded in 6-well plate at a density of 4×10^5 and siRNAs were transfected twice at 24 h intervals, using Effectene reagent (Qiagen) according to manufacturer's protocol. Five days after the first transfection, cells were deprived of serum overnight and were induced for 6 h with 10 nM Angiotensin II.

For induction of Wnt pathway activity, Y1 cells were seeded in 6-well plate at a density of 3×10^5 cells per well and cultured in minimum medium overnight, before treatment with 500 nM BIO (B1686, Sigma) or DMSO (control group) in the presence or absence of 100 nM actinomycin D for the indicated amount of time. For TOP/FOP-FLASH assays, 3×10^5 Y1 cells were transfected with 1 μg of each plasmid using Metafectene (Biontex) in complete medium for 6–7 h. They were then cultured in minimum medium overnight and treated with DMSO or BIO as described above, for 6 h.

Reverse-transcription quantitative PCR

Cells were harvested in lysis buffer and total mRNAs were extracted using RNAII nucleotide extraction kit (Macherey Nagel) according to manufacturer's instructions. One microgram of mRNA was reverse transcribed for 1 h at 42°C with 5 pmol of random hexamers primers, 200 units reverse transcriptase (M-MLV RT, M1701, Promega), 2 mM dNTPs and 20 units RNAsin (N2615, Promega). One microliter of a one-tenth dilution of cDNA was used in each quantitative PCR. This was conducted with Taqman® probes of the Gene Expression Assay pool (Applied Biosystems, see below) or MESA GREEN Mastermix Plus (RT-SY2X-06+WOUFL, Eurogentec). Primers and probes are listed in Supplementary Material, Tables S2 and S3.

Western blot

Thirty micrograms of total proteins were loaded on a 10% SDS–PAGE gel, transferred onto nitrocellulose and detected with an antibody to β-catenin 1/1000 (610153, BD Biosciences Pharmingen), NURR1 1/500 (sc-991, Santa Cruz) and NUR77 1/1000 (sc-990, Santa Cruz). Expression of these proteins was normalized to expression of β-actin (A2066, Sigma) and signals were quantified with a DNR MF ChemiBis 3.2 camera and Multi Gauge software suite (Fujifilm).

Chromatin immunoprecipitation

H295R cells were seeded at a density of 5×10^6 per 10 cm dish and treated with 1.0 μM PKF115-584 for 30 h. Following treatment, they were fixed by addition of 1% formaldehyde to the culture medium for 10 min. Fixation was stopped by addition of 125 μM glycine. Cells were rinsed three times with PBS and scraped in CLB buffer (5 mM PIPES, 85 mM KCl, 0.5% NP40). After centrifugation, nuclei pellet was resuspended in NLB buffer (50 mM Tris–HCl, 10 mM EDTA, 1% SDS) and incubated on ice for 45 min. Chromatin was then sheared to an average length of 500 pb and submitted to immunoprecipitation with 5 μg of antibodies directed against β-catenin (610153, BD Biosciences Pharmingen), NURR1 (sc-991, Santa Cruz), NUR77 (sc-990, Santa Cruz) or non-immune IgG controls (Millipore). Chromatin-antibodies complexes were collected with protein A or G magnetic beads (Dynabeads, Invitrogen). After seven washes in IP buffer (150 mM NaCl, 50 mM Tris–HCl, 5 mM EDTA, 0.5% NP40, 1% Triton X-100), beads were resuspended in 100 μl of 10% Chelex slurry and DNA was recovered as previously described (65).

For *in vivo* ChIP, six WT or ΔCat adrenals gland were cross-linked in PBS with 1% formaldehyde for 10 min at room temperature. Fixation was stopped with 125 μM glycine and adrenals were rinsed three times with PBS. Tissues were then disrupted in CLB with a glass tissue grinder. The next steps of the protocol were as described above for H295R cells. Primer pairs used for ChIP are listed in Supplementary Material, Table S4. For all ChIP experiments, specificity controls were performed with primers hybridizing within the coding sequence of each candidate gene (Supplementary Material, Table S4).

Hormone measurement

Aldosterone, DHEA, cortisol and corticosterone were quantified in plasma and cell medium using an aldosterone ELISA kit (CAN-ALD-450, Diagnostic Biochem Canada), a DHEA

ELISA kit (CAN-DH-490, Diagnostic Biochem Canada), a Cortisol ELISA kit (CAN-C-270, Diagnostic Biochem Canada) and a corticosterone 3H kit (MP Biomedicals) according to manufacturers' instructions. For cell medium quantifications, hormone concentrations were normalized to total cellular proteins measured by Bradford assays (Bio-Rad). Renin was measured by direct chemiluminescence with the Liaison Direct Renin kit (Diasorin), according to manufacturer's instructions.

SUPPLEMENTARY MATERIAL

Supplementary Material is available at *HMG* online.

ACKNOWLEDGEMENTS

We thank B. Terris at Cochin Tumour Bank and the COMETE (COrtico MEdullo Tumeurs Endocrines) network for the provision of APA tissue samples, Dr Brendan Lee (Baylor College of Medicine, Houston, USA) for kindly allowing us to use *Sfrp2* knockout mice, Dr William E Rainey (Medical college of Georgia, USA) for providing *CYP11B2* reporter constructs and Dr Ed Laufer (Columbia University, New York) for provision of antibodies. We also thank Khirredine Ouchen, Sandrine Plantade and Philippe Mazuel for animal care.

Conflict of Interest statement. None declared.

FUNDING

This work was supported through institutional support from Centre National de la Recherche Scientifique, Institut National de la Santé et de la Recherche Médicale; Université Blaise Pascal; Université d'Auvergne; Ministère de la Recherche et de l'Enseignement Supérieur and grants from Fondation ARC pour la Recherche sur le Cancer (SFI 20101201397; young researcher grant to A.B.); La Ligue Contre le Cancer, Allier committee; Agence Nationale pour la Recherche (013-01 and 08-GENO-021); Fondation pour la Recherche sur l'Hypertension Artérielle; Fondation pour la recherche médicale (ING20101221177) and Programme Hospitalier de Recherche Clinique (AOM 06179).

REFERENCES

1. Plouin, P.-F., Amar, L. and Chatellier, G. (2004) Trends in the prevalence of primary aldosteronism, aldosterone-producing adenomas, and surgically correctable aldosterone-dependent hypertension. *Nephrol. Dial. Transplant.*, **19**, 774–777.
2. Amar, L., Plouin, P.-F. and Steichen, O. (2010) Aldosterone-producing adenoma and other surgically correctable forms of primary aldosteronism. *Orphanet J. Rare Dis.*, **5**, 9.
3. Fagugli, R.M. and Taglioni, C. (2011) Changes in the perceived epidemiology of primary hyperaldosteronism. *Int. J. Hypertens.*, **2011**, 162804.
4. Steichen, O., Zinzindohoué, F., Plouin, P.-F. and Amar, L. (2012) Outcomes of adrenalectomy in patients with unilateral primary aldosteronism: a review. *Horm. Metab. Res.*, **44**, 221–227.
5. Rossi, G.P.D. (2011) Diagnosis and treatment of primary aldosteronism. *Rev. Endocr. Metab. Disord.*, **12**, 27–36.
6. Jeunemaitre, X., Chatellier, G., Kreft-Jais, C., Charru, A., DeVries, C., Plouin, P.F., Corvol, P. and Menard, J. (1987) Efficacy and tolerance of spironolactone in essential hypertension. *Am. J. Cardiol.*, **60**, 820–825.
7. Amar, L., Azizi, M., Menard, J., Peyrard, S., Watson, C. and Plouin, P.-F. (2010) Aldosterone synthase inhibition with LCI699: a proof-of-concept study in patients with primary aldosteronism. *Hypertension*, **56**, 831–838.
8. Calhoun, D.A., White, W.B., Krum, H., Guo, W., Bermann, G., Trapani, A., Lefkowitz, M.P. and Ménard, J. (2011) Effects of a novel aldosterone synthase inhibitor for treatment of primary hypertension: results of a randomized, double-blind, placebo- and active-controlled phase 2 trial. *Circulation*, **124**, 1945–1955.
9. Heitzmann, D., Derand, R., Jungbauer, S., Bandulik, S., Sterner, C., Schweda, F., El Wakil, A., Lalli, E., Guy, N., Mengual, R. *et al.* (2008) Invalidation of TASK1 potassium channels disrupts adrenal gland zonation and mineralocorticoid homeostasis. *EMBO J.*, **27**, 179–187.
10. Davies, L.A., Hu, C., Guagliardo, N.A., Sen, N., Chen, X., Talley, E.M., Carey, R.M., Bayliss, D.A. and Barrett, P.Q. (2008) TASK channel deletion in mice causes primary hyperaldosteronism. *Proc. Natl. Acad. Sci. USA*, **105**, 2203–2208.
11. Doi, M., Takahashi, Y., Komatsu, R., Yamazaki, F., Yamada, H., Haraguchi, S., Emoto, N., Okuno, Y., Tsujimoto, G., Kanematsu, A. *et al.* (2010) Salt-sensitive hypertension in circadian clock-deficient Cry-null mice involves dysregulated adrenal Hsd3b6. *Nat. Med.*, **16**, 67–74.
12. Oki, K., Plonczynski, M.W., Lam, M.L., Gomez-Sanchez, E.P. and Gomez-Sanchez, C.E. (2012) The potassium channel, Kir3.4 participates in Angiotensin II-stimulated aldosterone production by a human adrenocortical cell line. *Endocrinology*, **153**, 4328–4335.
13. Monticone, S., Hattangady, N.G., Nishimoto, K., Mantero, F., Rubin, B., Cicala, M.V., Pezzani, R., Auchus, R.J., Ghayee, H.K., Shibata, H. *et al.* (2012) Effect of KCNJ5 mutations on gene expression in aldosterone-producing adenomas and adrenocortical cells. *J. Clin. Endocrinol. Metab.*, **97**, E1567–E1572.
14. Choi, M., Scholl, U.I., Yue, P., Björklund, P., Zhao, B., Nelson-Williams, C., Ji, W., Cho, Y., Patel, A., Men, C.J. *et al.* (2011) K+ channel mutations in adrenal aldosterone-producing adenomas and hereditary hypertension. *Science*, **331**, 768–772.
15. Azizan, E.A.B., Lam, B.Y.H., Newhouse, S.J., Zhou, J., Kuc, R.E., Clarke, J., Happerfield, L., Marker, A., Hoffman, G.J. and Brown, M.J. (2012) Microarray, qPCR, and KCNJ5 sequencing of aldosterone-producing adenomas reveal differences in genotype and phenotype between zona glomerulosa- and zona fasciculata-like tumors. *J. Clin. Endocrinol. Metab.*, **97**, E819–E829.
16. Beuschlein, F., Boulkroun, S., Osswald, A., Wieland, T., Nielsen, H.N., Lichtenauer, U.D., Penton, D., Schack, V.R., Amar, L., Fischer, E. *et al.* (2013) Somatic mutations in ATP1A1 and ATP2B3 lead to aldosterone-producing adenomas and secondary hypertension. *Nat. Genet.*, 10.1038/ng.2550.
17. Boulkroun, S., Beuschlein, F., Rossi, G.-P., Golib-Dzib, J.-F., Fischer, E., Amar, L., Mulatero, P., Samson-Couterie, B., Hahner, S., Quinkler, M. *et al.* (2012) Prevalence, clinical, and molecular correlates of KCNJ5 mutations in primary aldosteronism. *Hypertension*, **59**, 592–598.
18. Åkerström, T., Crona, J., Delgado Verdugo, A., Starker, L.F., Cupisti, K., Willenberg, H.S., Knoefel, W.T., Saeger, W., Feller, A., Ip, J. *et al.* (2012) Comprehensive re-sequencing of adrenal aldosterone producing lesions reveal three somatic mutations near the KCNJ5 potassium channel selectivity filter. *PLoS ONE*, **7**, e41926.
19. Berthon, A., Sahut-Barnola, I., Lambert-Langlais, S., de Joussineau, C., Damon-Soubeyrand, C., Louiset, E., Taketo, M.M., Tissier, F., Bertherat, J., Lefrancois-Martinez, A.M. *et al.* (2010) Constitutive {beta}-catenin activation induces adrenal hyperplasia and promotes adrenal cancer development. *Hum. Mol. Genet.*, **19**, 1561–1576.
20. Berthon, A., Martinez, A., Bertherat, J. and Val, P. (2011) Wnt/β-catenin signalling in adrenal physiology and tumour development. *Mol. Cell. Endocrinol.*, **351**, 87–95.
21. Boulkroun, S., Samson-Couterie, B., Golib-Dzib, J.-F., Amar, L., Plouin, P.-F., Sibony, M., Lefebvre, H., Louiset, E., Jeunemaitre, X., Meatchi, T. *et al.* (2011) Aldosterone-producing adenoma formation in the adrenal cortex involves expression of stem/progenitor cell markers. *Endocrinology*, **152**, 4753–4763.
22. De Reynies, A., Assie, G., Rickman, D.S., Tissier, F., Groussin, L., Rene-Corail, F., Dousset, B., Bertagna, X., Clauser, E. and Bertherat, J. (2009) Gene expression profiling reveals a new classification of adrenocortical tumors and identifies molecular predictors of malignancy and survival. *J. Clin. Oncol.*, **27**, 1108–1115.
23. Suzuki, H., Watkins, D.N., Jair, K.W., Schuebel, K.E., Markowitz, S.D., Chen, W.D., Pretlow, T.P., Yang, B., Akiyama, Y., Van Engeland, M. *et al.*

(2004) Epigenetic inactivation of SFRP genes allows constitutive WNT signaling in colorectal cancer. *Nat. Genet.*, **36**, 417–422.
24. Morello, R., Bertin, T.K., Schlaubitz, S., Shaw, C.A., Kakuru, S., Munivez, E., Hermanns, P., Chen, Y., Zabel, B. and Lee, B. (2008) Brachy-syndactyly caused by loss of Sfrp2 function. *J. Cell. Physiol.*, **217**, 127–137.
25. Romero, D.G., Yanes, L.L., de Rodriguez, A.F., Plonczynski, M.W., Welsh, B.L., Reckelhoff, J.F., Gomez-Sanchez, E.P. and Gomez-Sanchez, C.E. (2007) Disabled-2 is expressed in adrenal zona glomerulosa and is involved in aldosterone secretion. *Endocrinology*, **148**, 2644–2652.
26. Tissier, F., Cavard, C., Groussin, L., Perlemoine, K., Fumey, G., Hagnere, A.M., Rene-Corail, F., Jullian, E., Gicquel, C., Bertagna, X. *et al.* (2005) Mutations of beta-catenin in adrenocortical tumors: activation of the Wnt signaling pathway is a frequent event in both benign and malignant adrenocortical tumors. *Cancer Res.*, **65**, 7622–7627.
27. Lepourcelet, M., Chen, Y.N., France, D.S., Wang, H., Crews, P., Petersen, F., Bruseo, C., Wood, A.W. and Shivdasani, R.A. (2004) Small-molecule antagonists of the oncogenic Tcf/beta-catenin protein complex. *Cancer Cell*, **5**, 91–102.
28. Bassett, M.H., Suzuki, T., Sasano, H., White, P.C. and Rainey, W.E. (2004) The orphan nuclear receptors NURR1 and NGFIB regulate adrenal aldosterone production. *Mol. Endocrinol.*, **18**, 279–290.
29. Wu, H., Lin, Y., Li, W., Sun, Z., Gao, W., Zhang, H., Xie, L., Jiang, F., Qin, B., Yan, T. *et al.* (2011) Regulation of Nur77 expression by beta-catenin and its mitogenic effect in colon cancer cells. *FASEB J.*, **25**, 192–205.
30. Ragazzon, B., Libe, R., Gaujoux, S., Assie, G., Fratticci, A., Launay, P., Clauser, E., Bertagna, X., Tissier, F., de Reynies, A. *et al.* (2010) Transcriptome analysis reveals that p53 and {beta}-catenin alterations occur in a group of aggressive adrenocortical cancers. *Cancer Res.*, **70**, 8276–8281.
31. Gaujoux, S., Grabar, S., Fassnacht, M., Ragazzon, B., Launay, P., Libe, R., Chokri, I., Audebourg, A., Royer, B., Sbiera, S. *et al.* (2011) beta-catenin activation is associated with specific clinical and pathologic characteristics and a poor outcome in adrenocortical carcinoma. *Clin. Cancer Res.*, **17**, 328–336.
32. Bonnet, S., Gaujoux, S., Launay, P., Baudry, C., Chokri, I., Ragazzon, B., Libe, R., Rene-Corail, F., Audebourg, A., Vacher-Lavenu, M.C. *et al.* (2011) Wnt/beta-catenin pathway activation in adrenocortical adenomas is frequently due to somatic CTNNB1-activating mutations, which are associated with larger and nonsecreting tumors: a study in cortisol-secreting and -nonsecreting tumors. *J. Clin. Endocrinol. Metab.*, **96**, E419–E426.
33. Tadjine, M., Lampron, A., Ouadi, L., Horvath, A., Stratakis, C.A. and Bourdeau, I. (2008) Detection of somatic beta-catenin mutations in primary pigmented nodular adrenocortical disease. *Clin. Endocrinol. (Oxf.)*, **69**, 367–373.
34. Li, Q., Ishikawa, T.-O., Oshima, M. and Taketo, M.M. (2005) The threshold level of adenomatous polyposis coli protein for mouse intestinal tumorigenesis. *Cancer Res.*, **65**, 8622–8627.
35. Kielman, M.F., Rindapää, M., Gaspar, C., van Poppel, N., Breukel, C., van Leeuwen, S., Taketo, M.M., Roberts, S., Smits, R. and Fodde, R. (2002) Apc modulates embryonic stem-cell differentiation by controlling the dosage of beta-catenin signaling. *Nat. Genet.*, **32**, 594–605.
36. Albuquerque, C., Breukel, C., van der Luijt, R., Fidalgo, P., Lage, P., Slors, F.J.M., Leitão, C.N., Fodde, R. and Smits, R. (2002) The 'just-right' signaling model: APC somatic mutations are selected based on a specific level of activation of the beta-catenin signaling cascade. *Hum. Mol. Genet.*, **11**, 1549–1560.
37. Buchert, M., Athineos, D., Abud, H.E., Burke, Z.D., Faux, M.C., Samuel, M.S., Jarnicki, A.G., Winbanks, C.E., Newton, I.P., Meniel, V.S. *et al.* (2010) Genetic dissection of differential signaling threshold requirements for the Wnt/beta-catenin pathway in vivo. *PLoS Genet.*, **6**, e1000816.
38. Benhamouche, S., Decaens, T., Godard, C., Chambrey, R., Rickman, D.S., Moinard, C., Vasseur-Cognet, M., Kuo, C.J., Kahn, A., Perret, C. *et al.* (2006) Apc tumor suppressor gene is the 'zonation-keeper' of mouse liver. *Dev. Cell*, **10**, 759–770.
39. Bovolenta, P., Esteve, P., Ruiz, J.M., Cisneros, E. and Lopez-Rios, J. (2008) Beyond Wnt inhibition: new functions of secreted Frizzled-related proteins in development and disease. *J. Cell. Sci.*, **121**, 737–746.
40. Nojima, M., Suzuki, H., Toyota, M., Watanabe, Y., Maruyama, R., Sasaki, S., Sasaki, Y., Mita, H., Nishikawa, N., Yamaguchi, K. *et al.* (2007) Frequent epigenetic inactivation of SFRP genes and constitutive activation of Wnt signaling in gastric cancer. *Oncogene*, **26**, 4699–4713.
41. Suzuki, H., Toyota, M., Carraway, H., Gabrielson, E., Ohmura, T., Fujikane, T., Nishikawa, N., Sogabe, Y., Nojima, M., Sonoda, T. *et al.* (2008) Frequent epigenetic inactivation of Wnt antagonist genes in breast cancer. *Br. J. Cancer*, **98**, 1147–1156.
42. Hassan, M.Q., Maeda, Y., Taipaleenmaki, H., Zhang, W., Jafferji, M., Gordon, J.A.R., Li, Z., Croce, C.M., van Wijnen, A.J., Stein, J.L. *et al.* (2012) miR-218 directs a Wnt signaling circuit to promote differentiation of osteoblasts and osteomimicry of metastatic cancer cells. *J. Biol. Chem.*, **287**, 42084–42092.
43. Kapinas, K., Kessler, C., Ricks, T., Gronowicz, G. and Delany, A.M. (2010) miR-29 modulates Wnt signaling in human osteoblasts through a positive feedback loop. *J. Biol. Chem.*, **285**, 25221–25231.
44. Snyder, C.M., Rice, A.L., Estrella, N.L., Held, A., Kandarian, S.C. and Naya, F.J. (2013) MEF2A regulates the Gtl2-Dio3 microRNA mega-cluster to modulate WNT signaling in skeletal muscle regeneration. *Development*, **140**, 31–42.
45. Fu, J., Tang, W., Du, P., Wang, G., Chen, W., Li, J., Zhu, Y., Gao, J. and Cui, L. (2012) Identifying microRNA-mRNA regulatory network in colorectal cancer by a combination of expression profile and bioinformatics analysis. *BMC Syst. Biol.*, **6**, 68.
46. Kim, A.C., Reuter, A.L., Zubair, M., Else, T., Serecky, K., Bingham, N.C., Lavery, G.G., Parker, K.L. and Hammer, G.D. (2008) Targeted disruption of beta-catenin in Sf1-expressing cells impairs development and maintenance of the adrenal cortex. *Development*, **135**, 2593–2602.
47. Heikkila, M., Peltoketo, H., Leppaluoto, J., Ilves, M., Vuolteenaho, O. and Vainio, S. (2002) Wnt-4 deficiency alters mouse adrenal cortex function, reducing aldosterone production. *Endocrinology*, **143**, 4358–4365.
48. Chen, M. and Hornsby, P.J. (2006) Adenovirus-delivered DKK3/WNT4 and steroidogenesis in primary cultures of adrenocortical cells. *Horm. Metab. Res.*, **38**, 549–555.
49. Roy, L., McDonald, C.A., Jiang, C., Maroni, D., Zeleznik, A.J., Wyatt, T.A., Hou, X. and Davis, J.S. (2009) Convergence of 3′,5′-cyclic adenosine 5′-monophosphate/protein kinase A and glycogen synthase kinase-3beta/beta-catenin signaling in corpus luteum progesterone synthesis. *Endocrinology*, **150**, 5036–5045.
50. Parakh, T.N., Hernandez, J.A., Grammer, J.C., Weck, J., Hunzicker-Dunn, M., Zeleznik, A.J. and Nilson, J.H. (2006) Follicle-stimulating hormone/cAMP regulation of aromatase gene expression requires beta-catenin. *Proc. Natl. Acad. Sci. USA*, **103**, 12435–12440.
51. Boyer, A., Goff, A.K. and Boerboom, D. (2010) WNT signaling in ovarian follicle biology and tumorigenesis. *Trends Endocrinol. Metab.*, **21**, 25–32.
52. Boyer, A., Lapointe, E., Zheng, X., Cowan, R.G., Li, H., Quirk, S.M., DeMayo, F.J., Richards, J.S. and Boerboom, D. (2010) WNT4 is required for normal ovarian follicle development and female fertility. *FASEB J.*, **24**, 3010–3025.
53. Hernandez Gifford, J.A., Hunzicker-Dunn, M.E. and Nilson, J.H. (2009) Conditional deletion of beta-catenin mediated by Amhr2cre in mice causes female infertility. *Biol. Reprod.*, **80**, 1282–1292.
54. Sun, Z., Cao, X., Jiang, M.-M., Qiu, Y., Zhou, H., Chen, L., Qin, B., Wu, H., Jiang, F., Chen, J. *et al.* (2012) Inhibition of β-catenin signaling by nongenomic action of orphan nuclear receptor Nur77. *Oncogene*, **31**, 2653–2667.
55. Rajalin, A.-M. and Aarnisalo, P. (2011) Cross-talk between NR4A orphan nuclear receptors and β-catenin signaling pathway in osteoblasts. *Arch. Biochem. Biophys.*, **509**, 44–51.
56. Lee, S.-O., Abdelrahim, M., Yoon, K., Chintharlapalli, S., Papineni, S., Kim, K., Wang, H. and Safe, S. (2010) Inactivation of the orphan nuclear receptor TR3/Nur77 inhibits pancreatic cancer cell and tumor growth. *Cancer Res.*, **70**, 6824–6836.
57. Kolluri, S.K., Bruey-Sedano, N., Cao, X., Lin, B., Lin, F., Han, Y.-H., Dawson, M.I. and Zhang, X. (2003) Mitogenic effect of orphan receptor TR3 and its regulation by MEKK1 in lung cancer cells. *Mol. Cell. Biol.*, **23**, 8651–8667.
58. Ke, N., Claassen, G., Yu, D.-H., Albers, A., Fan, W., Tan, P., Grifman, M., Hu, X., Defife, K., Nguy, V. *et al.* (2004) Nuclear hormone receptor NR4A2 is involved in cell transformation and apoptosis. *Cancer Res.*, **64**, 8208–8212.
59. Shan, B.E., Wang, M.X. and Li, R.Q. (2009) Quercetin inhibit human SW480 colon cancer growth in association with inhibition of cyclin D1 and survivin expression through Wnt/beta-catenin signaling pathway. *Cancer Invest.*, **27**, 604–612.
60. Russo, M., Spagnuolo, C., Tedesco, I., Bilotto, S. and Russo, G.L. (2012) The flavonoid quercetin in disease prevention and therapy: facts and fancies. *Biochem. Pharmacol.*, **83**, 6–15.

61. Romero, M., Jiménez, R., Hurtado, B., Moreno, J.M., Rodríguez-Gómez, I., López-Sepúlveda, R., Zarzuelo, A., Pérez-Vizcaino, F., Tamargo, J., Vargas, F. *et al.* (2010) Lack of beneficial metabolic effects of quercetin in adult spontaneously hypertensive rats. *Eur. J. Pharmacol.*, **627**, 242–250.
62. Larson, A.J., Symons, J.D. and Jalili, T. (2012) Therapeutic potential of quercetin to decrease blood pressure: review of efficacy and mechanisms. *Adv. Nutr.*, **3**, 39–46.
63. Takahashi-Yanaga, F. and Kahn, M. (2010) Targeting Wnt signaling: can we safely eradicate cancer stem cells? *Clin. Cancer Res.*, **16**, 3153–3162.
64. Drelon, C., Berthon, A., Ragazzon, B., Tissier, F., Bandiera, R., Sahut-Barnola, I., De Joussineau, C., Batisse-Lignier, M., Lefrançois-Martinez, A.-M., Bertherat, J. *et al.* (2012) Analysis of the role of Igf2 in adrenal tumour development in transgenic mouse models. *PLoS ONE*, **7**, e44171.
65. Nelson, J.D., Denisenko, O. and Bomsztyk, K. (2006) Protocol for the fast chromatin immunoprecipitation (ChIP) method. *Nat. Protoc.*, **1**, 179–185.